

Identification of novel SNPs associated with coronary artery disease and birth weight using a pleiotropic cFDR method

Xinrui Wu¹, Xu Lin², Qi Li³, Zun Wang⁴, Na Zhang¹, Mengyuan Tian¹, Xiaolei Wang¹, Hongwen Deng^{5,6}, Hongzhuan Tan¹

¹Department of Epidemiology and Health Statistics, Xiangya School of Public Health, Central South University, Changsha 410078, China

²Department of Endocrinology and Metabolism, The Third Affiliated Hospital of Southern Medical University, Guangzhou 510630, China

³Xiangxi Center for Disease Prevention and Control, Jishou 416000, China

⁴Xiangya Nursing School, Central South University, Changsha 410013, China

⁵School of Basic Medical Science, Central South University, Changsha 410013, China

⁶Tulane Center for Biomedical Informatics and Genomics, School of Medicine, Tulane University, New Orleans, LA 70112, USA

Correspondence to: Hongzhuan Tan; email: tanhz@csu.edu.cn

Keywords: coronary artery disease, birth weight, conditional FDR, pleiotropy, Mendelian randomization

Received: September 19, 2020 **Accepted:** November 11, 2020 **Published:** December 19, 2020

Copyright: © 2020 Wu et al. This is an open access article distributed under the terms of the [Creative Commons Attribution License](https://creativecommons.org/licenses/by/3.0/) (CC BY 3.0), which permits unrestricted use, distribution, and reproduction in any medium, provided the original author and source are credited.

ABSTRACT

Objectives: Clinical and epidemiological findings indicate an association between coronary artery disease (CAD) and low birth weight (BW). However, the mechanisms underlying this relationship are largely unknown. Here, we aimed to identify novel single-nucleotide polymorphisms (SNPs) associated with CAD, BW, and their shared pleiotropic loci, and to detect the potential causal relationship between CAD and BW.

Methods: We first applied a genetic pleiotropic conditional false discovery rate (cFDR) method to two independent genome-wide association studies (GWAS) summary statistics of CAD and BW to estimate the pleiotropic enrichment between them. Then, bi-directional Mendelian randomization (MR) analyses were performed to clarify the causal association between these two traits.

Results: By incorporating related traits into a conditional analysis framework, we observed the significant pleiotropic enrichment between CAD and BW. By applying the cFDR level of 0.05, 109 variants were detected for CAD, 203 for BW, and 26 pleiotropic variants for both traits. We identified 11 CAD- and/or BW-associated SNPs that showed more than three of the metabolic quantitative trait loci (metaQTL), protein QTL (pQTL), methylation QTL (meQTL), or expression QTL (eQTL) effects. The pleiotropic SNP rs10774625, located at *ATXN2*, showed metaQTL, pQTL, meQTL, and eQTL effects simultaneously. Using the bi-directional MR approach, we found a negative association from BW to CAD (odds ratio [OR] = 0.68, 95% confidence interval [CI]: 0.59 to 0.80, $p = 1.57 \times 10^{-6}$).

Conclusion: We identified several pleiotropic loci between CAD and BW by leveraging GWAS results of related phenotypes and identified a potential causal relationship from BW to CAD. Our findings provide novel insights into the shared biological mechanisms and overlapping genetic heritability between CAD and BW.

INTRODUCTION

Coronary artery disease (CAD) is characterized by the narrowing or obstruction of the coronary arteries, which can lead to chest pain, arrhythmia, heart failure, and even permanent heart damage [1]. In 2017, over 485 million people suffered from CAD, resulting in 17.8 million deaths [2, 3], making this disease the leading cause of morbidity and mortality worldwide [4].

Numerous studies have shown that early life experiences, including low birth weight (BW), may increase the risk of cardiovascular diseases [5–7]. Thus, the World Health Organization has classified low BW as a risk factor for CAD later in life [8]. However, the prevalence of CAD does not decrease with higher BW accompanied by improved living conditions [9]. In addition, many randomized controlled trials designed to improve BW revealed different results [10, 11], leaving the relationship between BW and CAD unclear.

CAD and BW are highly influenced by multiple genetic factors with heritability estimates over 30–60% [12] and 30–50% [13], respectively. With the development of genome-wide association studies (GWAS), more than 230 CAD-associated [14–19] and 80 BW-associated loci [20–22] have been detected. These loci describe only a small part of the genetic contribution [23, 24], leaving a large proportion of “missing heritability” unexplained [25]. Pleiotropy occurs when one gene or variant affects multiple phenotypes [26]. Among the human genome, more than 17% of genes and 5% of single-nucleotide polymorphisms (SNPs) show pleiotropic effects [27]. Considering the potential causal relationship, large genetic determination, pleiotropic effect, and missing heritability between CAD and BW, it is necessary to illuminate biological mechanisms and uncover novel associated genetic variants for both traits.

By leveraging the pleiotropic effect in related traits, a conditional false discovery rate (cFDR) method was developed without additional subjects recruitment [28]. This approach is cost-effective and could improve the identification of novel genetic loci underlying missing heritability, thereby elucidating genetic mechanisms associated with multiple phenotypes [29–32]. Furthermore, Mendelian randomization (MR) is an approach to investigate the potential causality between exposure and outcome using genetic instrumental variables [33]. As genetic variants are randomly distributed among the population and are generally independent of confounders, such analysis may reduce confounding bias and eliminate potential reversed causal relationship [34].

In this study, we applied cFDR and bi-directional MR analyses to two large and independent GWAS datasets aiming to 1) identify additional novel loci and the genetic pleiotropy of CAD and BW, and 2) estimate the causality between CAD and BW. Therefore, we can improve SNP detection, and clarify the shared mechanistic relationship and overlapping genetic heritability between these two traits better.

RESULTS

Pleiotropic enrichment estimation

We found leftward separations between each line (including the null line) in the stratified quantile-quantile (Q-Q) plots, which indicated the pleiotropy of CAD conditional on BW (Figure 1A), as well as BW conditional on CAD (Figure 1B). As shown in fold-enrichment plots (Figure 1C, 1D), distinct upward shifts from the baseline demonstrated a strong pleiotropic enrichment between BW and CAD. We observed the most notable pleiotropy with an enrichment fold greater than 40 in BW conditional on CAD.

Furthermore, the stratified Q-Q plots for CAD conditional on autism spectrum disorder (ASD) (Supplementary Figure 1A), and BW conditional on ASD (Supplementary Figure 1C) all showed no enrichment and vice versa (Supplementary Figure 1B, 1D), which can be the negative controls.

CAD-associated SNPs identified by cFDR

Conditional on BW, we identified 109 significant SNPs (cFDR ≤ 0.05) associated with CAD variation, which were located on 20 different chromosomes (1–17, 19, 21–22), annotated to 98 genes (Supplementary Table 1 and Figure 2A). We validated 22 SNPs that were statistically significant in the former CAD GWAS datasets [14–19]. Additionally, six SNPs associated with cardiovascular function were also validated in our research [35–38]. Excluding 26 SNPs that showed high linkage disequilibrium (LD) ($r^2 > 0.6$) with the previous CAD-related loci, the remaining 55 SNPs were potentially novel to CAD (Supplementary Table 2). Using validation datasets, we found 111 significant SNPs for CAD, 73 of which (65.8%) were also significant in the original cFDR research (Supplementary Table 3).

We detected 16 SNPs associated with various metabolites (Supplementary Table 7), such as kynurenine, C18:1 sphingomyelin, and cholesterol, which affected the pathogenesis of CAD. Seven SNPs were associated with different proteins, and 27 SNPs showed significant metabolic quantitative trait locus (metaQTL) effects in

the human serum. Notably, three novel SNPs, rs11244035, rs3811417, and rs624249, showed more than three metaQTL, protein QTL (pQTL), methylation QTL (meQTL), or expression QTL (eQTL) effects simultaneously (Table 1).

BW-associated SNPs identified by cFDR

Conditional on CAD, we identified 203 significant SNPs ($cFDR \leq 0.05$) associated with BW variation, which were located on 22 chromosomes (1–22), annotated to 179 genes (Supplementary Table 4 and Figure 2B). We validated 27 SNPs that were statistically significant in the former BW GWAS

datasets [20–22, 39], although 19 of the remaining 176 SNPs showed high LD ($r^2 > 0.6$) with the previous BW-related loci (Supplementary Table 5). Using validation datasets, we found 229 significant SNPs for BW, 182 of which (79.5%) were also significant in the original cFDR research (Supplementary Table 6).

We detected 26 SNPs associated with various metabolites (Supplementary Table 7), five were associated with different proteins, and 31 showed significant meQTL effects in the human serum. In particular, four novel SNPs, rs143384, rs4875812, rs6700896, and rs8108865, showed more than three metaQTL, pQTL, meQTL, or eQTL effects simultaneously (Table 1).

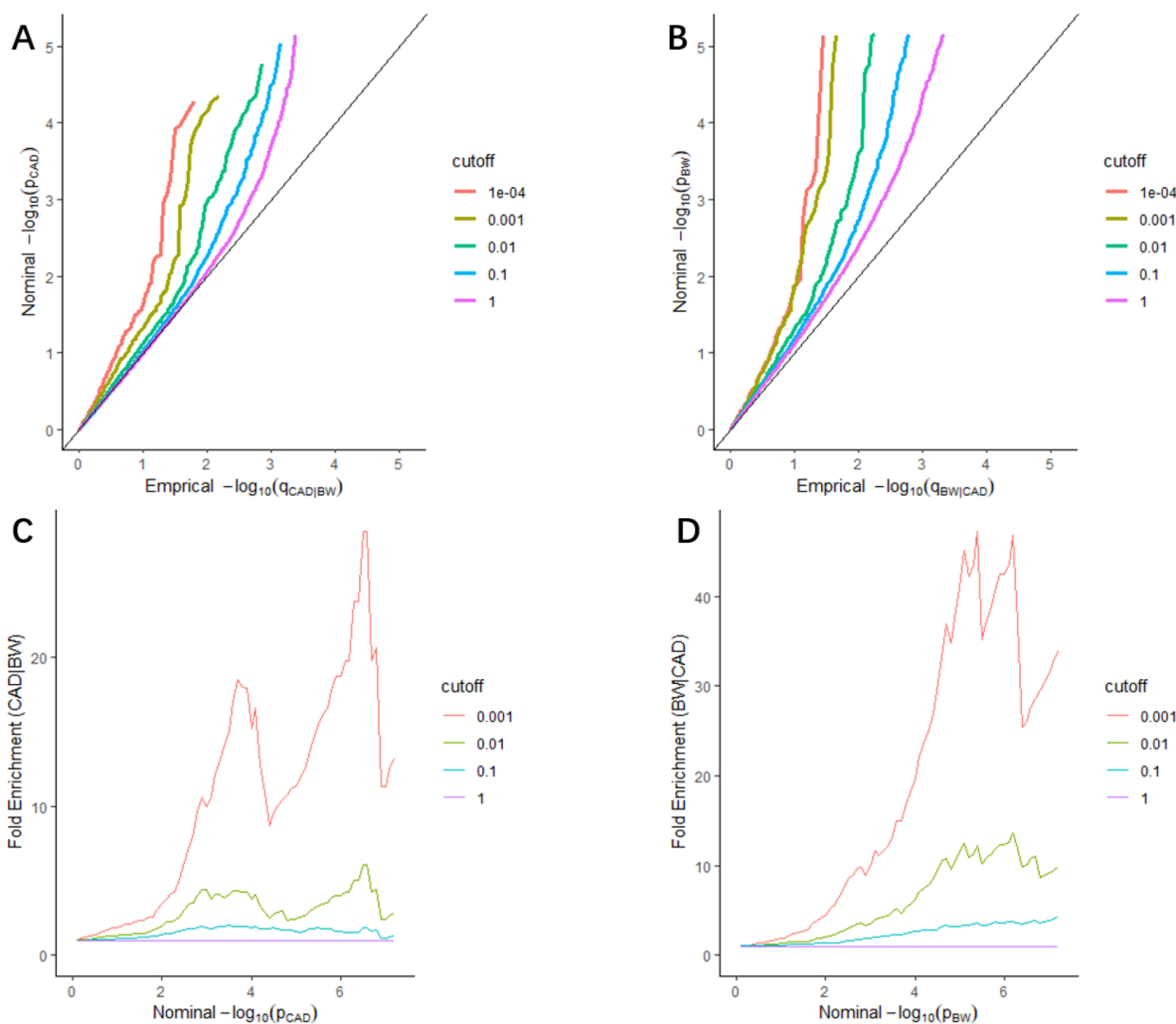


Figure 1. Stratified Q-Q plots and fold-enrichment plots. Stratified Q-Q plots of nominal vs. empirical $-\log_{10}(p)$ values in principal trait below the standard GWAS threshold of $p \leq 5 \times 10^{-8}$ as a function of the significance of the association with conditional trait at the level of $p \leq 1$, $p \leq 0.1$, $p \leq 0.01$, $p \leq 0.001$, and $p \leq 0.0001$, respectively. (A) CAD as a function of the significance of the association with BW, and (B) BW as a function of the significance of the association with CAD. Fold-enrichment plots of enrichment vs nominal $-\log_{10}(p)$ values (corrected for inflation) corresponding to levels of $p \leq 1$, $p \leq 0.1$, $p \leq 0.01$, $p \leq 0.001$, respectively in (C) CAD below the standard GWAS threshold of $p \leq 5 \times 10^{-8}$ as a function of significance of the association with BW; and in (D) BW below the standard GWAS threshold of $p \leq 5 \times 10^{-8}$ as a function of significance with CAD. Dashed lines indicate the null-hypothesis.

Potentially pleiotropic SNPs identified using conjunction cFDR (ccFDR)

We calculated the ccFDR value and constructed the conjunction Manhattan plot to explore the pleiotropic loci between CAD and BW. (Figure 2C). Precisely 26 potentially pleiotropic loci that reached a significance threshold at $\text{ccFDR} \leq 0.05$ were mapped to 13 chromosomes and annotated to 26 different genes. We validated three SNPs that were statistically significant in the original GWAS and CAD-related study, nine loci were also found to be related to other phenotypes (Supplementary Table 8). Using validation datasets, we found 17 pleiotropic SNPs for both traits, 12 of which

(70.5%) were also pleiotropic loci in the original ccFDR research (Supplementary Table 9). We then detected 18 pleiotropic SNPs that showed more than one of the metaQTL, pQTL, meQTL, or eQTL effects. Particularly, rs10774625 showed all QTL effects simultaneously (Table 2).

Causality between BW and CAD

After instrument selection, LD clumping, variant extraction, and harmonization, 52 BW-CAD SNP pairs were selected when choosing BW as exposure (Supplementary Table 10). The MR-Egger regression test result (intercept: -0.0025, 95% confidence interval

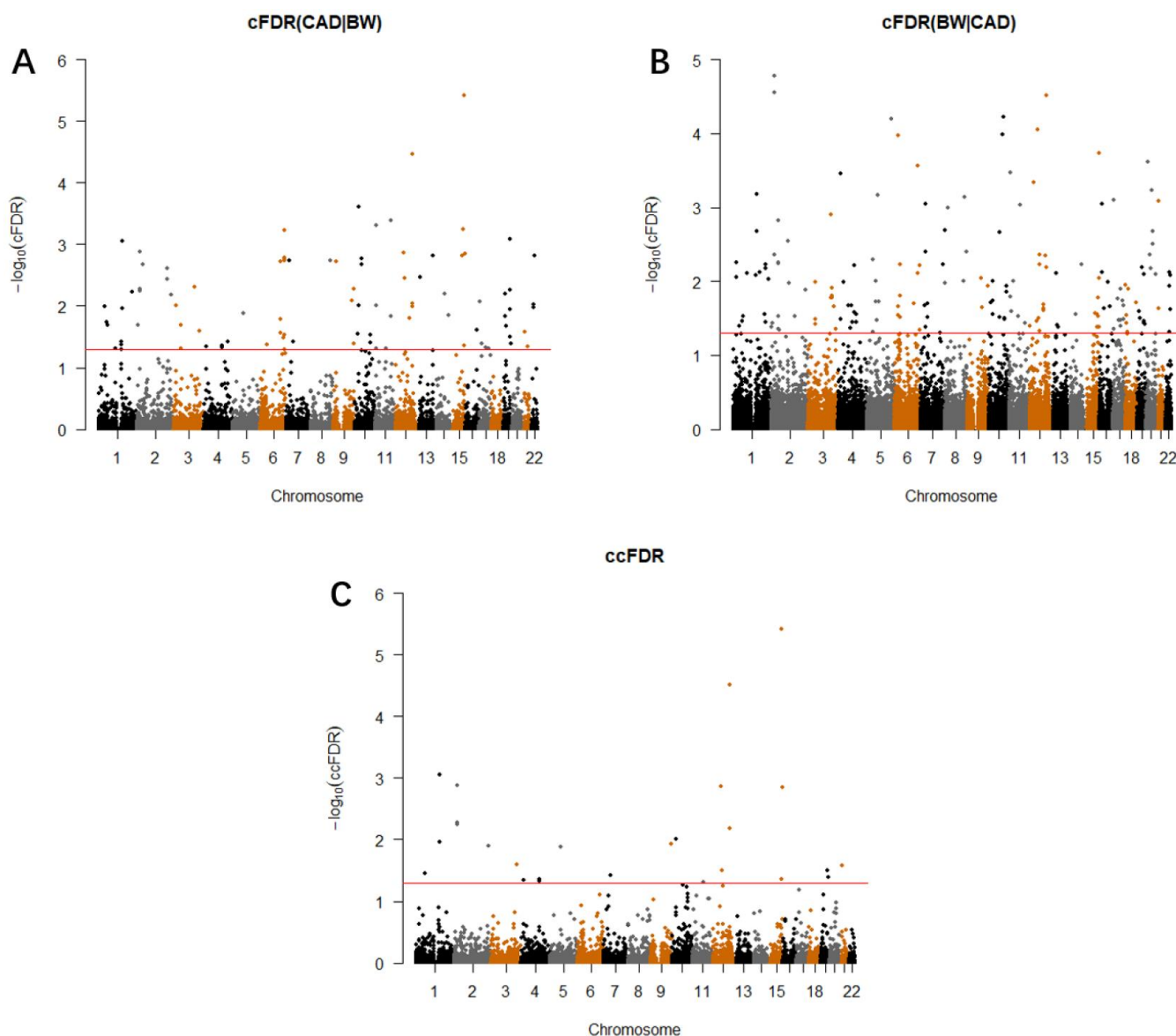


Figure 2. Conditional Manhattan plot. SNPs with $-\log_{10}(\text{cFDR}) \geq 1.3$ ($\text{cFDR} \leq 0.05$) for (A) CAD given BW (CAD|BW) and (B) BW given CAD (BW|CAD), or (C) $-\log_{10}(\text{ccFDR}) \geq 1.3$ ($\text{ccFDR} \leq 0.05$) are shown above the red line.

Table 1. Conjunction cFDR for 26 pleiotropic SNPs in CAD and BW (ccFDR ≤ 0.05).

SNP	Chr	Pos	Alt	Gene	Annotation	metaQTL/pQTL/meQTL/eQTL	SNP Type	Gene Type	cFDR_CA D	cFDR_BW	ccFDR
rs10774625	12	111472415	A/T	<i>ATXN2</i>	intronic	metaQTL/pQTL/meQTL/eQTL(3 hits)	CAD	CAD	1.48E-08	3.06E-05	3.06E-05
rs11066301	12	112433568	A/T	<i>PTPN11</i>	intronic	metaQTL/meQTL/eQTL(1 hit)	CAD	CAD	3.45E-05	6.50E-03	6.50E-03
rs11172113	12	57133500	T/A	<i>LRP1</i>	intronic	metaQTL/meQTL/eQTL(4 hits)	Novel	Novel	3.56E-03	3.18E-02	3.18E-02
rs11206803	1	56411837	C/G	<i>AC119674.2</i>	intronic	meQTL	Novel	Novel	2.02E-02	3.51E-02	3.51E-02
rs12148530	15	96542056	T/A	<i>7SK</i>	intergenic		Novel	Novel	4.40E-02	1.64E-02	4.40E-02
rs12306172	12	54145221	G/C	<i>SMUG1</i>	intronic	eQTL(7 hits)	Novel	Novel	1.37E-03	8.89E-05	1.37E-03
rs13035774	2	24135782	C/G	<i>FAM228B</i>	intronic	meQTL/eQTL(29 hits)	Novel	Novel	5.73E-03	4.35E-03	5.73E-03
rs1319869	15	98669256	G/C	<i>IGF1R</i>	intronic		Novel	BW	1.41E-03	1.85E-04	1.41E-03
rs1480933	4	119512093	C/G	<i>PDE5A</i>	intronic	pQTL/eQTL(17 hits)	Novel	Novel	4.43E-02	3.52E-02	4.43E-02
rs1861044	4	15537875	A/T	<i>CC2D2A</i>	intronic	pQTL	Novel	Novel	4.54E-02	3.25E-02	4.54E-02
rs2268310	7	44637499	C/G	<i>OGDH</i>	intronic	meQTL	Novel	Novel	3.85E-02	3.10E-02	3.85E-02
rs2339940	2	24028917	G/C	<i>MFS2B</i>	intronic	eQTL(22 hits)	Novel	Novel	1.34E-03	1.67E-05	1.34E-03
rs3756668	5	68300260	G/C	<i>PIK3R1</i>	3'-UTR		Novel	Novel	1.32E-02	6.91E-04	1.32E-02
rs4233701	2	23706216	G/C	<i>KLHL29</i>	intronic	eQTL(15 hits)	Novel	Novel	5.26E-03	2.81E-05	5.26E-03
rs4643791	4	119344464	G/C	<i>FABP2</i>	intergenic	eQTL(21 hits)	Novel	Novel	4.76E-02	2.75E-02	4.76E-02
rs502467	3	172009573	T/A	<i>FND3B</i>	intergenic		Novel	Novel	2.58E-02	2.22E-02	2.58E-02
rs611003	11	69630516	C/G	<i>CCND1</i>	intergenic		Novel	Novel	4.98E-02	9.20E-04	4.98E-02
rs630014	9	133274306	A/T	<i>ABO</i>	intronic	metaQTL/meQTL/eQTL(9 hits)	Novel	CAD	5.22E-03	1.16E-02	1.16E-02
rs6673081	1	155017119	T/A	<i>ZBTB7B</i>	3'-UTR	eQTL(8 hits)	Novel	BW	8.98E-04	4.66E-08	8.98E-04
rs670950	19	43777410	T/A	<i>KCNN4</i>	intronic	eQTL(1 hit)	Novel	Novel	3.15E-02	7.91E-03	3.15E-02
rs6713510	2	226169783	G/C	<i>LOC646736</i>	intronic		CAD	CAD	6.65E-03	1.29E-02	1.29E-02
rs8039305	15	90879313	T/A	<i>FURIN</i>	intronic	meQTL/eQTL(27 hits)	Novel	CAD	3.77E-06	1.13E-06	3.77E-06
rs8105944	19	51047598	C/G	<i>KLK13</i>	intergenic		Novel	Novel	4.04E-02	3.81E-02	4.04E-02
rs821551	1	155718789	C/G	<i>DAP3</i>	intronic	meQTL/eQTL(50 hits)	Novel	Novel	1.08E-02	6.67E-04	1.08E-02
rs866919	10	30224354	C/G	<i>RP11</i>	intergenic	eQTL(1 hit)	Novel	Novel	9.93E-03	9.87E-03	9.93E-03
rs965098	21	15185306	G/C	<i>JCAD</i>	intergenic		Novel	Novel	2.64E-02	2.35E-02	2.64E-02

Abbreviations: Chr, chromosome; Pos, chromosomal position (GRCh38/hg38); metaQTL, metabolic quantitative trait locus; pQTL, protein quantitative trait locus; meQTL, methylation quantitative trait locus; eQTL, expression quantitative trait locus; CAD, coronary artery disease; BW, birth weight; cFDR, conditional false discovery rate; ccFDR, conjunctive conditional false discovery rate. The allele was exhibited as reference allele/alter allele; SNP type and gene type means whether identified SNPs and genes have been reported in previous GWAS or in previous related cFDR studies.

Table 2. Functional annotation for 11 SNPs showing significant effects in metaQTL, pQTL, meQTL, and eQTL.

SNP	GENCODE genes	Traits	metaQTL	pQTL	meQTL (P)	eQTL Hits	Promoter histone marks	Enhancer histone marks	DNase	Proteins bound	Motifs changed
rs10774625	<i>ATXN2</i>	Pleiotropic	9 hits	B2M	4.10E-16	3 hits					9 altered motifs
rs11066301	<i>PTPN11</i>	Pleiotropic	2 hits		6.48E-12	1 hit		BLD			6 altered motifs
rs11172113	<i>LRP1</i>	Pleiotropic	SM C18:1		1.43E-07	4 hits	8 tissues	15 tissues	17 tissues	FOXA1	AP-2, Hic1, PU.1
rs630014	<i>ABO</i>	Pleiotropic	2 hits		4.82E-09	9 hits	4 tissues	GI, MUS	ESC,GI		Gm397, RP58
rs11244035	<i>OBP2B</i>	CAD		8 hits	1.37E-05	6 hits					Ik-1, Ik-2, NERF1a
rs3811417	<i>RORC</i>	CAD	nonanoylcarnitine		5.46E-06	2 hits	5 tissues	12 tissues	CRVX		Arnt, Mxi1, Myc
rs624249	<i>SLC22A2</i>	CAD	X-12798		9.90E-05	3 hits		4 tissues			
rs143384	<i>GDF5</i>	BW		CPN1	1.27E-07	47 hits	9 tissues	13 tissues	16 tissues		Ascl2
rs4875812	<i>MIR596</i>	BW	deoxycholate		3.11E-12	3 hits		4 tissues			9 altered motifs
rs6700896	<i>LEPR</i>	BW		LEPR	3.16E-07	1 hit		LIV	SKIN,SKIN	CTCF	GR, Myf, TCF12
rs8108865	<i>FCHO1</i>	BW	HWESASXX		1.27E-28	1 hit		BRN, BLD			NF-Y, NF-kappaB, Pou2f2

Abbreviations: metaQTL, metabolic quantitative trait locus; pQTL, protein quantitative trait locus; meQTL, methylation quantitative trait locus; eQTL, expression quantitative trait locus; DNase, deoxyribonuclease; SM C18:1, C18:1 sphingomyelin; B2M, beta-2-microglobulin.

[CI]: -0.015 to 0.014, $p = 0.973$) suggested that there was no genetic confounding due to horizontal pleiotropy. The null-pleiotropy result was also confirmed using scatter plots and funnel plots (Supplementary Figures 2, 3). There was no apparent heterogeneity in our chosen SNPs, as evidenced by Cochran's Q test (Supplementary Table 11). We found a negative association of BW to CAD from the inverse-variance weighted (IVW) estimates (odds ratio [OR] = 0.68, 95% CI: 0.59 to 0.80, $p = 1.57 \times 10^{-6}$), which was consistent with all other MR methods (Table 3 and Figure 3). MR leave-one-out sensitivity analysis demonstrated that there was no influence of outlying and/or pleiotropic (Supplementary Figure 4). However, in the opposite direction, we found no causal relationship from CAD to BW (Supplementary Table 12).

Functional enrichment and protein-protein interaction analyses

We discovered significant enrichment of biological processes including "regulation of phospholipid metabolic process" ($p = 1.10 \times 10^{-4}$) and "negative regulation of lipid transport" ($p = 2.40 \times 10^{-4}$) for genes associated with CAD by conducting functional enrichment analysis. Moreover, genes associated with BW were enriched in gene ontology (GO) terms like "tube morphogenesis" ($p = 1.20 \times 10^{-4}$) and "regulation of multicellular organismal process" ($p = 3.10 \times 10^{-4}$). Interestingly, the results for pleiotropic variants showed a cluster of biological processes in insulin and kinase categories, which might contribute to body growth and the progression of CAD (Table 4).

According to the protein-protein interaction network for CAD (Supplementary Figure 5A), proteins such as *FURIN*, *FLT1*, *PLG*, *LDLR*, and *APOE* were closely connected, and have been demonstrated to affect cardiovascular function [14, 40–42]. Similarly, in the BW network (Supplementary Figure 5B), proteins including *ADRB1*, *ADCY5*, *ESR1*, *EPAS1*, and *CDKAL1* were closely connected and have been demonstrated to affect BW [21, 43–45].

DISCUSSION

In this study, we incorporated summary statistics from two independent GWAS datasets and discovered 109 and 203 SNPs associated with CAD and BW, respectively. By performing the ccFDR method, we further detected 26 pleiotropic loci associated with both phenotypes. Following a bi-directional MR analysis and functional annotation, we confirmed the causal relationship from BW to CAD and speculated the underlying shared genetic mechanisms between these two traits.

Notably, we identified 11 CAD- and/or BW-associated SNPs that showed more than three of the metaQTL, pQTL, meQTL, or eQTL effects. These functional loci might have a great effect on the pathogenesis of CAD and/or BW. For example, rs11172113 is located in the intron of *LRPI*, a member of the low-density lipoprotein receptor family, which regulates extracellular proteolytic activities [46]. *LRPI* plays a pivotal role in mediating inflammation and efferocytosis [47], and mouse studies have shown that *LRPI* knockout leads to diminished vessel integrity and high-density lipoprotein secretion [48]. Another study proved that *LRPI* regulates food intake and energy homeostasis by acting as a co-activator of PPAR γ [49]. Moreover, the lipidomic analysis demonstrated that the metabolite C18:1 sphingomyelin, which is associated with rs11172113, was enhanced in CAD patients compared to that in the control group [50]. Another longitudinal prospective study revealed that the alteration of sphingomyelin metabolism is associated with BW percentiles [51], suggesting a potentially crucial role for this SNP in both traits.

Furthermore, we identified one pleiotropic locus, rs10774625, showing metaQTL, pQTL, eQTL, and meQTL effects simultaneously. rs10774625 is located in the intron of *ATXN2*. One population-based GWAS demonstrated that the *ATXN2-SH3* region contributes to changes in the retinal venular caliber, an endophenotype of the microcirculation related to clinical cardiovascular diseases [52]. Animal experiments supported the role of *ATXN2* in translational regulation as well as embryonic development [53]. Another *ATXN2* knockdown experiment demonstrated that mice lacking *ATXN2* develop dysfunction in energy metabolism and weight regulation [54, 55]. It has been reported that rs10774625 is associated with the kynurenine metabolite pathway (KP) [56]. Evidence indicates that the activation of indoleamine 2,3-dioxygenase, the inducible enzyme in KP, is closely limited by endothelial cells [57], vascular smooth muscle cells [58], and dendritic cells [59], all of which play vital roles in cardiac pathophysiology [60]. Epidemiologically, it was shown that the concentration of kynurenine is associated with body weight indexes in a European cohort of more than 1000 people [61]. An immunohistochemistry study also detected that the kynurenine-to-tryptophan ratio limits the expression of inflammatory markers in the adipose tissue, which is correlated with body weight [62]. In addition, beta-2-microglobulin (B2M) is associated with rs10774625, which reduces the capacity for energy conversion and restricts intrauterine growth, resulting in low BW [63], and is also implicated in the pathogenesis of CAD [64]. These facts indicated that rs10774625 (representing gene *ATXN2*) might be essential in linking the pathogenesis between CAD and BW.

Table 3. Causal relationship from BW to CAD by Mendelian randomization analysis.

Method	nSNP	OR (95%CI)	P_value
Simple median	52	0.72 (0.61, 0.84)	2.89E-05
Weighted median	52	0.68 (0.62, 0.76)	1.33E-13
Weighted mode	52	0.70 (0.55, 0.89)	6.34E-03
Maximum likelihood	52	0.69 (0.62, 0.76)	8.57E-13
MR Egger	52	0.63 (0.39, 1.01)	6.22E-02
Inverse variance weighted	52	0.68 (0.59, 0.80)	1.57E-06

Abbreviations: nSNP, number of SNPs applied in the test; OR, odds ratio; 95%CI, 95% confidence interval. Detailed SNPs information are exhibited in Supplementary Table 10.

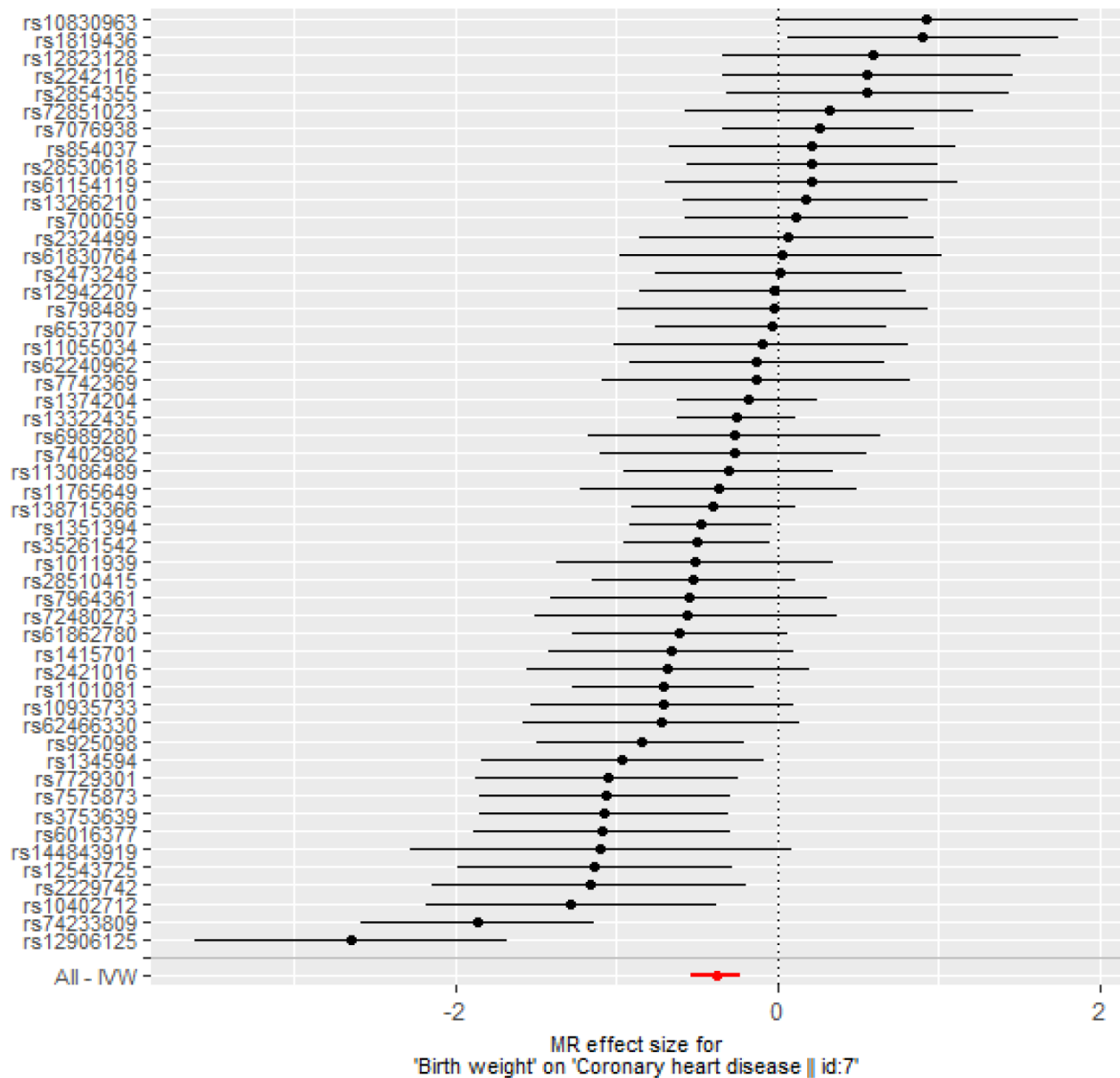


Figure 3. Forest plot of MR estimates BW on CAD. The estimated causal effect of BW on CAD was expressed by IVW (OR= 0.68, 95% CI: 0.59 to 0.80, $p = 1.57 \times 10^{-6}$).

Table 4. Gene ontology (GO) terms enriched for SNP-annotated genes with FDR ≤ 0.05.

Traits	GO terms	Term description	Gene counts	FDR
CAD	GO:1903725	regulation of phospholipid metabolic process	7	1.10E-04
	GO:0032369	negative regulation of lipid transport	5	2.40E-04
	GO:0019220	regulation of phosphate metabolic process	22	2.70E-04
	GO:0032375	negative regulation of cholesterol transport	4	2.70E-04
	GO:0051241	negative regulation of multicellular organismal process	18	2.70E-04
BW	GO:0035239	tube morphogenesis	19	1.20E-04
	GO:0051239	regulation of multicellular organismal process	42	3.10E-04
	GO:0030154	cell differentiation	47	4.30E-04
	GO:0035295	tube development	20	4.30E-04
	GO:0072359	circulatory system development	20	4.30E-04
Pleiotropic	GO:0043560	insulin receptor substrate binding	3	1.20E-04
	GO:0005158	insulin receptor binding	3	4.30E-04
	GO:0043559	insulin binding	2	2.20E-03
	GO:0016538	cyclin-dependent protein serine/threonine kinase regulator activity	2	3.60E-02
	GO:0043548	phosphatidylinositol 3-kinase binding	2	3.60E-02

According to the functional enrichment results, we could also hypothesize the possible shared pathogenesis mechanisms between CAD and BW. GO terms including “regulation of phospholipid metabolic process”, “regulation of multicellular organismal process”, and “insulin receptor binding,” have important impacts on metabolic abnormalities, such as impaired fasting glucose [65], dyslipidemia, and hypertension [66], which could contribute to the increased risk for both traits.

Our study has some strengths. First, we improved the identification of potential CAD- and BW-associated SNPs and detected several pleiotropic loci in both traits. Following MR analysis, we assessed the causal effect between these two related traits. Second, we took into account ASD, which is unlikely to be correlated with CAD and BW, for a “control trait” enrichment analysis, which provided a baseline to examine pleiotropic enrichment and statistically validate the novel findings in our study. Third, evidence from metaQTL, pQTL, eQTL, and meQTL effects suggested a possible explanation for the etiology of CAD and/or BW and improved the interpretability of the results.

Additionally, our study includes some limitations. First, we were unable to link the genetic findings to clinical measures due to the lack of raw datasets for individual clinical outcomes. However, our study aimed to identify potential novel SNPs and explore the overlapping biological mechanisms between CAD and BW. We hope that our findings can be validated via functional experiments or fine-mapping studies. Second, although we confirmed the causal relationship from BW to CAD,

the causalities of metabolomics, proteomics, and methylation between these two traits are unclear. Nevertheless, this problem could be solved by a follow-up multivariable MR study.

CONCLUSIONS

In conclusion, by applying the cFDR and bi-directional MR analyses to two strongly associated traits, we detected significant pleiotropic SNPs of potential functions for CAD and/or BW and estimated the causal relationship from BW to CAD. These findings provide a better understanding of the shared genetic mechanisms between CAD and BW, which might suggest a novel research direction for early disease prevention and subsequent treatment.

MATERIALS AND METHODS

GWAS data sources

The first CAD GWAS was obtained from the Coronary Artery Disease Genome-wide Replication and Meta-analysis plus The Coronary Artery Disease Genetics (CARDIoGRAMplusC4D) Consortium. This meta-analysis of 48 multiple ancestry studies involved more than 8.6 million SNPs from 60,801 cases and 123,504 controls [18]. The first BW dataset conducted by the Early Growth Genetics (EGG) Consortium consisted of 45 multiple ancestry studies including 321,223 subjects. As the control trait, the ASD dataset, collected by the Psychiatric Genomics Consortium, contained 15,954 participants with European ancestry (7,387 ASD cases and 8,567 controls) [67]. For validation, two other CAD

and BW datasets were used. The validation CAD dataset, comprising 10,801 cases and 137,914 controls, was collected by the CARDIoGRAMplusC4D Consortium [17]. The validation BW dataset, including 153,781 subjects, was collected by the EGG Consortium [21]. All datasets contained the summary statistics of each locus and the conducted genomic control [17, 18, 21, 22, 67].

cFDR and ccFDR for identifying shared variants

Data processing

First, two GWAS datasets were combined and 8,285,296 common SNPs with summary statistics remained for both CAD and BW phenotypes. Then, we performed LD-based pruning ($r^2 \leq 0.2$) using HapMap III genotypes as a reference, and the SNP of the pair with longer allele frequency was retained [31, 68]. After merging and pruning, 141,779 variants were prepared for further analysis.

Pleiotropic enrichment evaluation

We constructed stratified Q-Q plots to estimate the pleiotropic enrichment in two related phenotypes using the “ggplot2” R package. In this study, $-\log_{10}(p)$ which means the nominal p -value and $-\log_{10}(q)$ which means the empirical quantile were plotted on the Y- and X-axes, respectively, at different significance levels ($p \leq 1$, $p \leq 0.1$, $p \leq 0.01$, $p \leq 0.001$, and $p \leq 0.0001$). Under the null hypothesis, plots would fall on the line $Y=X$, and the enrichment of pleiotropic loci could be evaluated by the degree of leftward deviation from the null line. Additionally, we constructed fold-enrichment plots as a supplement for the Q-Q plots. Fold-enrichment and $-\log_{10}(p)$ were plotted on the Y- and X-axes, respectively, at different significance levels ($p \leq 1$, $p \leq 0.1$, $p \leq 0.01$, and $p \leq 0.001$) for CAD and BW. Pleiotropy could be visually observed via an upward deflection from the baseline (for the group including all SNPs ($p = 1$)).

Calculation of cFDR and ccFDR values

The cFDR method was used to estimate the possibility that a random SNP was not associated with the primary trait, given that its strength for the conditional traits was below the threshold [28]. This was an extension of the original FDR framework, applied for the cross-trait analysis [69]. Specifically, we computed cFDR for each SNP, selecting CAD as the primary phenotype given its association with BW (CAD|BW) and vice versa (BW|CAD). To detect the pleiotropic loci for both traits, we calculated the ccFDR value, the maximum of the two cFDR values. The ccFDR value indicated that the possibility that a given SNP was false positively related to two traits (CAD and BW) simultaneously. The thresholds for cFDR and ccFDR were set at 0.05.

Detailed steps of this approach have been described by Andreassen et al. [29].

Bi-directional MR analysis

To determine the relationship between BW and CAD, we performed a bi-directional MR analysis using the “TwoSampleMR” R package [70]. First, SNPs that were genome-wide significant ($p \leq 5 \times 10^{-8}$) in the exposure GWAS dataset were selected as genetic variants. To ensure that the instruments for exposure were independent, we performed LD-based clumping ($r^2 > 0.001$) and only retained the SNP with a lower p -value [68, 71]. Then, we extracted summary-level statistics for each selected SNP from the outcome trait and removed the SNPs related to the outcome phenotype ($p \leq 5 \times 10^{-8}$). The summary associations of candidate genetic variants were harmonized as described previously [72]. Finally, MR was conducted using IVW, simple median, weighted median, weighted mode, maximum likelihood, and MR-Egger approaches. BW and CAD were used as exposure and outcome measures, respectively, to identify the causal direction. The datasets used in the MR analysis were the same as that in the original cFDR analysis (The first CAD and BW datasets). To investigate whether any SNP had an outlying and/or pleiotropic influence, we also performed a leave-one-out sensitivity analysis.

Functional annotation and protein-protein interaction analyses

Online tools HaploReg (<http://compbio.mit.edu/HaploReg>) and RegulomeDB (<http://www.regulomedb.org/>) were applied to map each of the identified significant SNPs to nearby genes, corresponding DNA features, and regulatory elements. Next, we detected whether they possessed metaQTL, pQTL, meQTL, or eQTL effects. To obtain the metaQTL and pQTL hits, we applied the web-based software SNIIPA (<http://www.snipa.org/>), meQTL and eQTL information were collected from Bonder’s study [73] and HaploReg, respectively.

We used the GOEAST software to detect statistically overrepresented GO terms within the selected gene sets [74]. Meanwhile, using the STRING database, we conducted protein-protein interaction analyses to investigate the interaction and functional relationships of the identified CAD- and/or BW-related genes [75].

AUTHOR CONTRIBUTIONS

Xinrui Wu conceived the study, performed data analysis, interpretation and wrote the manuscript. Xu Lin, Qi Li, and Zun Wang were responsible for data collection and analysis. Na Zhang and Mengyuan Tian

contributed to the manuscript. Xiaolei Wang conducted experiments. Hongwen Deng gave constructive suggestions during the whole process. Hongzhan Tan provided guidance in study design, organized the investigation and is the corresponding author. All authors have read and approved the final manuscript before submission.

CONFLICTS OF INTEREST

The authors declare that they have no conflicts of interest.

FUNDING

This research was supported by the National Natural Science Foundation of China [No.81373088, No.81773535], China Scholarship Council [No.201806371067], the graduate student scientific research innovation project of Central South University [2019zzts328], the National Institutes of Health [R01AR069055, U19AG055373, P20GM109036, R01AG061917], and the Edward G. Schlieder Endowment fund from Tulane University.

REFERENCES

1. Thomas H, Diamond J, Vieco A, Chaudhuri S, Shinnar E, Cromer S, Perel P, Mensah GA, Narula J, Johnson CO, Roth GA, Moran AE. Global atlas of cardiovascular disease 2000-2016: the path to prevention and control. *Glob Heart*. 2018; 13:143–63. <https://doi.org/10.1016/j.gheart.2018.09.511> PMID:30301680
2. GBD 2017 Disease and Injury Incidence and Prevalence Collaborators. Global, regional, and national incidence, prevalence, and years lived with disability for 354 diseases and injuries for 195 countries and territories, 1990-2017: a systematic analysis for the global burden of disease study 2017. *Lancet*. 2018; 392:1789–858. [https://doi.org/10.1016/S0140-6736\(18\)32279-7](https://doi.org/10.1016/S0140-6736(18)32279-7) PMID:30496104
3. GBD 2017 Causes of Death Collaborators. Global, regional, and national age-sex-specific mortality for 282 causes of death in 195 countries and territories, 1980-2017: a systematic analysis for the global burden of disease study 2017. *Lancet*. 2018; 392:1736–88. [https://doi.org/10.1016/S0140-6736\(18\)32203-7](https://doi.org/10.1016/S0140-6736(18)32203-7) PMID:30496103
4. Benjamin EJ, Blaha MJ, Chiuve SE, Cushman M, Das SR, Deo R, de Ferranti SD, Floyd J, Fornage M, Gillespie C, Isasi CR, Jiménez MC, Jordan LC, et al, and American Heart Association Statistics Committee and Stroke Statistics Subcommittee. Heart disease and stroke statistics-2017 update: a report from the American heart association. *Circulation*. 2017; 135:e146–603. <https://doi.org/10.1161/CIR.0000000000000485> PMID:28122885
5. Gluckman PD, Hanson MA, Bateson P, Beedle AS, Law CM, Bhutta ZA, Anokhin KV, Bougnères P, Chandak GR, Dasgupta P, Smith GD, Ellison PT, Forrester TE, et al. Towards a new developmental synthesis: adaptive developmental plasticity and human disease. *Lancet*. 2009; 373:1654–57. [https://doi.org/10.1016/S0140-6736\(09\)60234-8](https://doi.org/10.1016/S0140-6736(09)60234-8) PMID:19427960
6. Sun D, Wang T, Heianza Y, Huang T, Shang X, Lv J, Li S, Harville E, Chen W, Fonseca V, Qi L. Birthweight and cardiometabolic risk patterns in multiracial children. *Int J Obes (Lond)*. 2018; 42:20–27. <https://doi.org/10.1038/ijo.2017.196> PMID:28925411
7. Tam CH, Wang Y, Luan J, Lee HM, Luk AO, Tutino GE, Tong PC, Ko GT, Ozaki R, Tam WH, Kong AP, So WY, Chan JC, Ma RC. Non-linear relationship between birthweight and cardiometabolic risk factors in Chinese adolescents and adults. *Diabet Med*. 2015; 32:220–25. <https://doi.org/10.1111/dme.12630> PMID:25388749
8. Organization WH. Strategic priorities of the WHO Cardiovascular Disease programme. https://www.who.int/cardiovascular_diseases/priorities/en
9. Chung RY, Schooling CM, Cowling BJ, Leung GM. How does socioeconomic development affect risk of mortality? an age-period-cohort analysis from a recently transitioned population in China. *Am J Epidemiol*. 2010; 171:345–56. <https://doi.org/10.1093/aje/kwp378> PMID:20042438
10. Nossier SA, Naeim NE, El-Sayed NA, Abu Zeid AA. The effect of zinc supplementation on pregnancy outcomes: a double-blind, randomised controlled trial, Egypt. *Br J Nutr*. 2015; 114:274–85. <https://doi.org/10.1017/S000711451500166X> PMID:26099195
11. Potdar RD, Sahariah SA, Gandhi M, Kehoe SH, Brown N, Sane H, Dayama M, Jha S, Lawande A, Coakley PJ, Marley-Zagar E, Chopra H, Shivshankaran D, et al. Improving women’s diet quality preconceptionally and during gestation: effects on birth weight and prevalence of low birth weight—a randomized controlled efficacy trial in India (Mumbai maternal nutrition project). *Am J Clin Nutr*. 2014; 100:1257–68. <https://doi.org/10.3945/ajcn.114.084921> PMID:25332324
12. Andreassen OA, Djurovic S, Thompson WK, Schork AJ, Kendler KS, O’Donovan MC, Rujescu D, Werge T, van de Bunt M, Morris AP, McCarthy MI, Roddey JC, McEvoy LK, et al, and International Consortium for

- Blood Pressure GWAS, and Diabetes Genetics Replication and Meta-analysis Consortium, and Psychiatric Genomics Consortium Schizophrenia Working Group. Improved detection of common variants associated with schizophrenia by leveraging pleiotropy with cardiovascular-disease risk factors. *Am J Hum Genet.* 2013; 92:197–209.
<https://doi.org/10.1016/j.ajhg.2013.01.001>
PMID:23375658
13. Clausson B, Lichtenstein P, Cnattingius S. Genetic influence on birthweight and gestational length determined by studies in offspring of twins. *BJOG.* 2000; 107:375–81.
<https://doi.org/10.1111/j.1471-0528.2000.tb13234.x>
PMID:10740335
 14. Deloukas P, Kanoni S, Willenborg C, Farrall M, Assimes TL, Thompson JR, Ingelsson E, Saleheen D, Erdmann J, Goldstein BA, Stirrups K, König IR, Cazier JB, et al, and CARDIoGRAMplusC4D Consortium, and DIAGRAM Consortium, and CARDIOGENICS Consortium, and MuTHER Consortium, and Wellcome Trust Case Control Consortium. Large-scale association analysis identifies new risk loci for coronary artery disease. *Nat Genet.* 2013; 45:25–33.
<https://doi.org/10.1038/ng.2480> PMID:23202125
 15. Coronary Artery Disease (C4D) Genetics Consortium. A genome-wide association study in europeans and south Asians identifies five new loci for coronary artery disease. *Nat Genet.* 2011; 43:339–44.
<https://doi.org/10.1038/ng.782> PMID:21378988
 16. Howson JM, Zhao W, Barnes DR, Ho WK, Young R, Paul DS, Waite LL, Freitag DF, Fauman EB, Salfati EL, Sun BB, Eicher JD, Johnson AD, et al, and CARDIoGRAM-plusC4D, and EPIC-CVD. Fifteen new risk loci for coronary artery disease highlight arterial-wall-specific mechanisms. *Nat Genet.* 2017; 49:1113–19.
<https://doi.org/10.1038/ng.3874> PMID:28530674
 17. Nelson CP, Goel A, Butterworth AS, Kanoni S, Webb TR, Marouli E, Zeng L, Ntalla I, Lai FY, Hopewell JC, Giannakopoulou O, Jiang T, Hamby SE, et al, EPIC-CVD Consortium, and CARDIoGRAMplusC4D, and UK Biobank CardioMetabolic Consortium CHD working group. Association analyses based on false discovery rate implicate new loci for coronary artery disease. *Nat Genet.* 2017; 49:1385–91.
<https://doi.org/10.1038/ng.3913> PMID:28714975
 18. Nikpay M, Goel A, Won HH, Hall LM, Willenborg C, Kanoni S, Saleheen D, Kyriakou T, Nelson CP, Hopewell JC, Webb TR, Zeng L, Dehghan A, et al. A comprehensive 1,000 genomes-based genome-wide association meta-analysis of coronary artery disease. *Nat Genet.* 2015; 47:1121–30.
<https://doi.org/10.1038/ng.3396> PMID:26343387
 19. Schunkert H, König IR, Kathiresan S, Reilly MP, Assimes TL, Holm H, Preuss M, Stewart AF, Barbalic M, Gieger C, Absher D, Aherrahrou Z, Allayee H, et al, and Cardiogenics, and CARDIoGRAM Consortium. Large-scale association analysis identifies 13 new susceptibility loci for coronary artery disease. *Nat Genet.* 2011; 43:333–38.
<https://doi.org/10.1038/ng.784> PMID:21378990
 20. Freathy RM, Mook-Kanamori DO, Sovio U, Prokopenko I, Timpson NJ, Berry DJ, Warrington NM, Widen E, Hottenga JJ, Kaakinen M, Lange LA, Bradfield JP, Kerkhof M, et al, and Genetic Investigation of ANthropometric Traits (GIANT) Consortium, and Meta-Analyses of Glucose and Insulin-related traits Consortium, and Wellcome Trust Case Control Consortium, and Early Growth Genetics (EGG) Consortium. Variants in ADCY5 and near CCNL1 are associated with fetal growth and birth weight. *Nat Genet.* 2010; 42:430–35.
<https://doi.org/10.1038/ng.567> PMID:20372150
 21. Horikoshi M, Beaumont RN, Day FR, Warrington NM, Kooijman MN, Fernandez-Tajes J, Feenstra B, van Zuydam NR, Gaulton KJ, Grarup N, Bradfield JP, Strachan DP, Li-Gao R, et al, and CHARGE Consortium Hematology Working Group, and Early Growth Genetics (EGG) Consortium. Genome-wide associations for birth weight and correlations with adult disease. *Nature.* 2016; 538:248–52.
<https://doi.org/10.1038/nature19806>
PMID:27680694
 22. Warrington NM, Beaumont RN, Horikoshi M, Day FR, Helgeland Ø, Laurin C, Bacelis J, Peng S, Hao K, Feenstra B, Wood AR, Mahajan A, Tyrrell J, et al, and EGG Consortium. Maternal and fetal genetic effects on birth weight and their relevance to cardio-metabolic risk factors. *Nat Genet.* 2019; 51:804–14.
<https://doi.org/10.1038/s41588-019-0403-1>
PMID:31043758
 23. Magnus P, Gjessing HK, Skrondal A, Skjaerven R. Paternal contribution to birth weight. *J Epidemiol Community Health.* 2001; 55:873–77.
<https://doi.org/10.1136/jech.55.12.873>
PMID:11707480
 24. Zdravkovic S, Wienke A, Pedersen NL, Marenberg ME, Yashin AI, De Faire U. Heritability of death from coronary heart disease: a 36-year follow-up of 20 966 Swedish twins. *J Intern Med.* 2002; 252:247–54.
<https://doi.org/10.1046/j.1365-2796.2002.01029.x>
PMID:12270005
 25. Pei YF, Zhang L, Papasian CJ, Wang YP, Deng HW. On individual genome-wide association studies and their meta-analysis. *Hum Genet.* 2014; 133:265–79.
<https://doi.org/10.1007/s00439-013-1366-4>
PMID:24114349

26. Stearns FW. One hundred years of pleiotropy: a retrospective. *Genetics*. 2010; 186:767–73.
<https://doi.org/10.1534/genetics.110.122549>
PMID:[21062962](https://pubmed.ncbi.nlm.nih.gov/21062962/)
27. Sivakumaran S, Agakov F, Theodoratou E, Prendergast JG, Zgaga L, Manolio T, Rudan I, McKeigue P, Wilson JF, Campbell H. Abundant pleiotropy in human complex diseases and traits. *Am J Hum Genet*. 2011; 89:607–18.
<https://doi.org/10.1016/j.ajhg.2011.10.004>
PMID:[22077970](https://pubmed.ncbi.nlm.nih.gov/22077970/)
28. Andreassen OA, Thompson WK, Schork AJ, Ripke S, Mattingsdal M, Kelsoe JR, Kendler KS, O'Donovan MC, Rujescu D, Werge T, Sklar P, Chen CH, McEvoy L, et al, and Psychiatric Genomics Consortium (PGC), and Bipolar Disorder and Schizophrenia Working Groups. Improved detection of common variants associated with schizophrenia and bipolar disorder using pleiotropy-informed conditional false discovery rate. *PLoS Genet*. 2013; 9:e1003455.
<https://doi.org/10.1371/journal.pgen.1003455>
PMID:[23637625](https://pubmed.ncbi.nlm.nih.gov/23637625/)
29. Greenbaum J, Deng HW. A statistical approach to fine mapping for the identification of potential causal variants related to bone mineral density. *J Bone Miner Res*. 2017; 32:1651–58.
<https://doi.org/10.1002/jbmr.3154> PMID:[28425624](https://pubmed.ncbi.nlm.nih.gov/28425624/)
30. Hu Y, Tan LJ, Chen XD, Liu Z, Min SS, Zeng Q, Shen H, Deng HW. Identification of novel potentially pleiotropic variants associated with osteoporosis and obesity using the cFDR method. *J Clin Endocrinol Metab*. 2018; 103:125–38.
<https://doi.org/10.1210/jc.2017-01531>
PMID:[29145611](https://pubmed.ncbi.nlm.nih.gov/29145611/)
31. Lin X, Peng C, Greenbaum J, Li ZF, Wu KH, Ao ZX, Zhang T, Shen J, Deng HW. Identifying potentially common genes between dyslipidemia and osteoporosis using novel analytical approaches. *Mol Genet Genomics*. 2018; 293:711–23.
<https://doi.org/10.1007/s00438-017-1414-1>
PMID:[29327327](https://pubmed.ncbi.nlm.nih.gov/29327327/)
32. Zhang Q, Wu KH, He JY, Zeng Y, Greenbaum J, Xia X, Liu HM, Lv WQ, Lin X, Zhang WD, Xi YL, Shi XZ, Sun CQ, Deng HW. Novel common variants associated with obesity and type 2 diabetes detected using a cFDR method. *Sci Rep*. 2017; 7:16397.
<https://doi.org/10.1038/s41598-017-16722-6>
PMID:[29180724](https://pubmed.ncbi.nlm.nih.gov/29180724/)
33. Smith GD, Ebrahim S. 'Mendelian randomization': can genetic epidemiology contribute to understanding environmental determinants of disease? *Int J Epidemiol*. 2003; 32:1–22.
<https://doi.org/10.1093/ije/dyg070>
PMID:[12689998](https://pubmed.ncbi.nlm.nih.gov/12689998/)
34. Lawlor DA, Harbord RM, Sterne JA, Timpson N, Davey Smith G. Mendelian randomization: using genes as instruments for making causal inferences in epidemiology. *Stat Med*. 2008; 27:1133–63.
<https://doi.org/10.1002/sim.3034>
PMID:[17886233](https://pubmed.ncbi.nlm.nih.gov/17886233/)
35. Lv WQ, Zhang X, Zhang Q, He JY, Liu HM, Xia X, Fan K, Zhao Q, Shi XZ, Zhang WD, Sun CQ, Deng HW. Novel common variants associated with body mass index and coronary artery disease detected using a pleiotropic cFDR method. *J Mol Cell Cardiol*. 2017; 112:1–7.
<https://doi.org/10.1016/j.yjmcc.2017.08.011>
PMID:[28843344](https://pubmed.ncbi.nlm.nih.gov/28843344/)
36. Peng C, Shen J, Lin X, Su KJ, Greenbaum J, Zhu W, Lou HL, Liu F, Zeng CP, Deng WF, Deng HW. Genetic sharing with coronary artery disease identifies potential novel loci for bone mineral density. *Bone*. 2017; 103:70–77.
<https://doi.org/10.1016/j.bone.2017.06.016>
PMID:[28651948](https://pubmed.ncbi.nlm.nih.gov/28651948/)
37. Wang Z, Qiu C, Lin X, Zhao LJ, Liu Y, Wu X, Wang Q, Liu W, Li K, Deng HW, Tang SY, Shen H. Identification of novel functional CpG-SNPs associated with type 2 diabetes and coronary artery disease. *Mol Genet Genomics*. 2020; 295:607–19.
<https://doi.org/10.1007/s00438-020-01651-3>
PMID:[32162118](https://pubmed.ncbi.nlm.nih.gov/32162118/)
38. Zhang Q, Liu HM, Lv WQ, He JY, Xia X, Zhang WD, Deng HW, Sun CQ. Additional common variants associated with type 2 diabetes and coronary artery disease detected using a pleiotropic cFDR method. *J Diabetes Complications*. 2018; 32:1105–12.
<https://doi.org/10.1016/j.jdiacomp.2018.09.003>
PMID:[30270018](https://pubmed.ncbi.nlm.nih.gov/30270018/)
39. Zeng CP, Chen YC, Lin X, Greenbaum J, Chen YP, Peng C, Wang XF, Zhou R, Deng WM, Shen J, Deng HW. Increased identification of novel variants in type 2 diabetes, birth weight and their pleiotropic loci. *J Diabetes*. 2017; 9:898–907.
<https://doi.org/10.1111/1753-0407.12510>
PMID:[27896934](https://pubmed.ncbi.nlm.nih.gov/27896934/)
40. Brænne I, Civelek M, Vilne B, Di Narzo A, Johnson AD, Zhao Y, Reiz B, Codoni V, Webb TR, Foroughi Asl H, Hamby SE, Zeng L, Trégouët DA, et al, and Leducq Consortium CAD Genomics. Prediction of causal candidate genes in coronary artery disease loci. *Arterioscler Thromb Vasc Biol*. 2015; 35:2207–17.
<https://doi.org/10.1161/ATVBAHA.115.306108>
PMID:[26293461](https://pubmed.ncbi.nlm.nih.gov/26293461/)
41. Byars SG, Huang QQ, Gray LA, Bakshi A, Ripatti S, Abraham G, Stearns SC, Inouye M. Genetic loci associated with coronary artery disease harbor evidence of selection and antagonistic pleiotropy. *PLoS Genet*. 2017; 13:e1006328.

- <https://doi.org/10.1371/journal.pgen.1006328>
PMID:28640878
42. López-Mejías R, Corrales A, Vicente E, Robustillo-Villarino M, González-Juanatey C, Llorca J, Genre F, Remuzgo-Martínez S, Dierssen-Sotos T, Miranda-Filloo JA, Huaranga MA, Pina T, Blanco R, et al. Influence of coronary artery disease and subclinical atherosclerosis related polymorphisms on the risk of atherosclerosis in rheumatoid arthritis. *Sci Rep*. 2017; 7:40303.
<https://doi.org/10.1038/srep40303> PMID:28059143
43. Horikoshi M, Yaghoobkar H, Mook-Kanamori DO, Sovio U, Taal HR, Hennig BJ, Bradfield JP, St Pourcain B, Evans DM, Charoen P, Kaakinen M, Cousminer DL, Lehtimäki T, et al, and Meta-Analyses of Glucose- and Insulin-related traits Consortium (MAGIC), and Early Growth Genetics (EGG) Consortium. New loci associated with birth weight identify genetic links between intrauterine growth and adult height and metabolism. *Nat Genet*. 2013; 45:76–82.
<https://doi.org/10.1038/ng.2477> PMID:23202124
44. van der Valk RJ, Kreiner-Møller E, Kooijman MN, Guxens M, Stergiakouli E, Sääf A, Bradfield JP, Geller F, Hayes MG, Cousminer DL, Körner A, Thiering E, Curtin JA, et al, and Early Genetics and Lifecourse Epidemiology (EAGLE) Consortium, and Genetic Investigation of ANthropometric Traits (GIANT) Consortium, and Early Growth Genetics (EGG) Consortium. A novel common variant in DCST2 is associated with length in early life and height in adulthood. *Hum Mol Genet*. 2015; 24:1155–68.
<https://doi.org/10.1093/hmg/ddu510> PMID:25281659
45. Au Yeung SL, Lin SL, Li AM, Schooling CM. Birth weight and risk of ischemic heart disease: a mendelian randomization study. *Sci Rep*. 2016; 6:38420.
<https://doi.org/10.1038/srep38420> PMID:27924921
46. Lillis AP, Van Duyn LB, Murphy-Ullrich JE, Strickland DK. LDL receptor-related protein 1: unique tissue-specific functions revealed by selective gene knockout studies. *Physiol Rev*. 2008; 88:887–918.
<https://doi.org/10.1152/physrev.00033.2007>
PMID:18626063
47. Mueller PA, Zhu L, Tavori H, Huynh K, Giunzioni I, Stafford JM, Linton MF, Fazio S. Deletion of macrophage low-density lipoprotein receptor-related protein 1 (LRP1) accelerates atherosclerosis regression and increases C-C chemokine receptor type 7 (CCR7) expression in plaque macrophages. *Circulation*. 2018; 138:1850–63.
<https://doi.org/10.1161/CIRCULATIONAHA.117.031702> PMID:29794082
48. Boucher P, Gotthardt M, Li WP, Anderson RG, Herz J. LRP: role in vascular wall integrity and protection from atherosclerosis. *Science*. 2003; 300:329–32.
<https://doi.org/10.1126/science.1082095>
PMID:12690199
49. Mao H, Lockyer P, Li L, Ballantyne CM, Patterson C, Xie L, Pi X. Endothelial LRP1 regulates metabolic responses by acting as a co-activator of PPAR γ . *Nat Commun*. 2017; 8:14960.
<https://doi.org/10.1038/ncomms14960>
PMID:28393867
50. Chatterjee M, Rath D, Schlotterbeck J, Rheinlaender J, Walker-Allgaier B, Alnaggar N, Zdanyte M, Müller I, Borst O, Geisler T, Schäffer TE, Lämmerhofer M, Gawaz M. Regulation of oxidized platelet lipidome: implications for coronary artery disease. *Eur Heart J*. 2017; 38:1993–2005.
<https://doi.org/10.1093/eurheartj/ehx146>
PMID:28431006
51. Hellmuth C, Lindsay KL, Uhl O, Buss C, Wadhwa PD, Koletzko B, Entringer S. Association of maternal prepregnancy BMI with metabolomic profile across gestation. *Int J Obes (Lond)*. 2017; 41:159–69.
<https://doi.org/10.1038/ijo.2016.153> PMID:27569686
52. Ikram MK, Sim X, Jensen RA, Cotch MF, Hewitt AW, Ikram MA, Wang JJ, Klein R, Klein BE, Breteler MM, Cheung N, Liew G, Mitchell P, et al, and Global BPgen Consortium. Four novel loci (19q13, 6q24, 12q24, and 5q14) influence the microcirculation in vivo. *PLoS Genet*. 2010; 6:e1001184.
<https://doi.org/10.1371/journal.pgen.1001184>
PMID:21060863
53. Ciosk R, DePalma M, Priess JR. ATX-2, the *C. Elegans* ortholog of ataxin 2, functions in translational regulation in the germline. *Development*. 2004; 131:4831–41.
<https://doi.org/10.1242/dev.01352> PMID:15342467
54. Lastres-Becker I, Brodesser S, Lütjohann D, Azizov M, Buchmann J, Hintermann E, Sandhoff K, Schürmann A, Nowock J, Auburger G. Insulin receptor and lipid metabolism pathology in ataxin-2 knock-out mice. *Hum Mol Genet*. 2008; 17:1465–81.
<https://doi.org/10.1093/hmg/ddn035> PMID:18250099
55. Kiehl TR, Nechiporuk A, Figueroa KP, Keating MT, Huynh DP, Pulst SM. Generation and characterization of Sca2 (ataxin-2) knockout mice. *Biochem Biophys Res Commun*. 2006; 339:17–24.
<https://doi.org/10.1016/j.bbrc.2005.10.186>
PMID:16293225
56. Shin SY, Fauman EB, Petersen AK, Krumsiek J, Santos R, Huang J, Arnold M, Erte I, Forgetta V, Yang TP, Walter K, Menni C, Chen L, et al, and Multiple Tissue Human Expression Resource (MuTHER) Consortium. An atlas of genetic influences on human blood metabolites. *Nat Genet*. 2014; 46:543–50.
<https://doi.org/10.1038/ng.2982> PMID:24816252

57. Wang Q, Zhang M, Ding Y, Wang Q, Zhang W, Song P, Zou MH. Activation of NAD(P)H oxidase by tryptophan-derived 3-hydroxykynurenine accelerates endothelial apoptosis and dysfunction in vivo. *Circ Res*. 2014; 114:480–92.
<https://doi.org/10.1161/CIRCRESAHA.114.302113>
PMID:24281189
58. Niinisalo P, Oksala N, Levula M, Pelto-Huikko M, Järvinen O, Salenius JP, Kytömäki L, Soini JT, Kähönen M, Laaksonen R, Hurme M, Lehtimäki T. Activation of indoleamine 2,3-dioxygenase-induced tryptophan degradation in advanced atherosclerotic plaques: tampere vascular study. *Ann Med*. 2010; 42:55–63.
<https://doi.org/10.3109/07853890903321559>
PMID:19941414
59. Yun TJ, Lee JS, Machmach K, Shim D, Choi J, Wi YJ, Jang HS, Jung IH, Kim K, Yoon WK, Miah MA, Li B, Chang J, et al. Indoleamine 2,3-Dioxygenase-Expressing Aortic Plasmacytoid Dendritic Cells Protect against Atherosclerosis by Induction of Regulatory T Cells. *Cell Metab*. 2016; 24:886.
<https://doi.org/10.1016/j.cmet.2016.11.008>
PMID:27974180
60. Wang Y, Liu H, McKenzie G, Witting PK, Stasch JP, Hahn M, Changsirivathanathamrong D, Wu BJ, Ball HJ, Thomas SR, Kapoor V, Celermajer DS, Mellor AL, et al. Kynurenine is an endothelium-derived relaxing factor produced during inflammation. *Nat Med*. 2010; 16:279–85.
<https://doi.org/10.1038/nm.2092> PMID:20190767
61. Favennec M, Hennart B, Caiazza R, Leloire A, Yengo L, Verbanck M, Arredouani A, Marre M, Pigeyre M, Bessede A, Guillemin GJ, Chinetti G, Staels B, et al. The kynurenine pathway is activated in human obesity and shifted toward kynurenine monooxygenase activation. *Obesity (Silver Spring)*. 2015; 23:2066–74.
<https://doi.org/10.1002/oby.21199>
PMID:26347385
62. Wolowczuk I, Hennart B, Leloire A, Bessede A, Soichot M, Taront S, Caiazza R, Raverdy V, Pigeyre M, Guillemin GJ, Allorge D, Pattou F, Froguel P, Poulain-Godefroy O, and ABOS Consortium. Tryptophan metabolism activation by indoleamine 2,3-dioxygenase in adipose tissue of obese women: an attempt to maintain immune homeostasis and vascular tone. *Am J Physiol Regul Integr Comp Physiol*. 2012; 303:R135–43.
<https://doi.org/10.1152/ajpregu.00373.2011>
PMID:22592557
63. Wang KC, Lim CH, McMillen IC, Duffield JA, Brooks DA, Morrison JL. Alteration of cardiac glucose metabolism in association to low birth weight: experimental evidence in lambs with left ventricular hypertrophy. *Metabolism*. 2013; 62:1662–72.
<https://doi.org/10.1016/j.metabol.2013.06.013>
PMID:23928106
64. Yao C, Chen G, Song C, Keefe J, Mendelson M, Huan T, Sun BB, Laser A, Maranville JC, Wu H, Ho JE, Courchesne P, Lyass A, et al. Genome-wide mapping of plasma protein QTLs identifies putatively causal genes and pathways for cardiovascular disease. *Nat Commun*. 2018; 9:3268.
<https://doi.org/10.1038/s41467-018-05512-x>
PMID:30111768
65. Nielson C, Lange T, Hadjokas N. Blood glucose and coronary artery disease in nondiabetic patients. *Diabetes Care*. 2006; 29:998–1001.
<https://doi.org/10.2337/diacare.295998>
PMID:16644627
66. Karalis DG, Victor B, Ahedor L, Liu L. Use of lipid-lowering medications and the likelihood of achieving optimal LDL-cholesterol goals in coronary artery disease patients. *Cholesterol*. 2012; 2012:861924.
<https://doi.org/10.1155/2012/861924> PMID:22888414
67. Autism Spectrum Disorders Working Group of The Psychiatric Genomics Consortium. Meta-analysis of GWAS of over 16,000 individuals with autism spectrum disorder highlights a novel locus at 10q24.32 and a significant overlap with schizophrenia. *Mol Autism*. 2017; 8:21.
<https://doi.org/10.1186/s13229-017-0137-9>
PMID:28540026
68. Purcell S, Neale B, Todd-Brown K, Thomas L, Ferreira MA, Bender D, Maller J, Sklar P, de Bakker PI, Daly MJ, Sham PC. PLINK: a tool set for whole-genome association and population-based linkage analyses. *Am J Hum Genet*. 2007; 81:559–75.
<https://doi.org/10.1086/519795> PMID:17701901
69. Benjamini Y, Drai D, Elmer G, Kafkafi N, Golani I. Controlling the false discovery rate in behavior genetics research. *Behav Brain Res*. 2001; 125:279–84.
[https://doi.org/10.1016/s0166-4328\(01\)00297-2](https://doi.org/10.1016/s0166-4328(01)00297-2)
PMID:11682119
70. Hemani G, Zheng J, Elsworth B, Wade KH, Haberland V, Baird D, Laurin C, Burgess S, Bowden J, Langdon R, Tan VY, Yarmolinsky J, Shihab HA, et al. The MR-base platform supports systematic causal inference across the human phenome. *Elife*. 2018; 7:e34408.
<https://doi.org/10.7554/eLife.34408> PMID:29846171
71. Zhang Q, Greenbaum J, Zhang WD, Sun CQ, Deng HW. Age at menarche and osteoporosis: a mendelian randomization study. *Bone*. 2018; 117:91–97.
<https://doi.org/10.1016/j.bone.2018.09.015>
PMID:30240960
72. Hartwig FP, Davies NM, Hemani G, Davey Smith G. Two-sample mendelian randomization: avoiding the

downsides of a powerful, widely applicable but potentially fallible technique. *Int J Epidemiol.* 2016; 45:1717–26.

<https://doi.org/10.1093/ije/dyx028>

PMID:[28338968](https://pubmed.ncbi.nlm.nih.gov/28338968/)

73. Bonder MJ, Luijk R, Zhernakova DV, Moed M, Deelen P, Vermaat M, van Iterson M, van Dijk F, van Galen M, Bot J, Sliker RC, Jhamai PM, Verbiest M, et al, and BIOS Consortium. Disease variants alter transcription factor levels and methylation of their binding sites. *Nat Genet.* 2017; 49:131–38.

<https://doi.org/10.1038/ng.3721>

PMID:[27918535](https://pubmed.ncbi.nlm.nih.gov/27918535/)

74. Zheng Q, Wang XJ. GOEAST: a web-based software toolkit for gene ontology enrichment analysis. *Nucleic Acids Res.* 2008; 36:W358–63.

<https://doi.org/10.1093/nar/gkn276> PMID:[18487275](https://pubmed.ncbi.nlm.nih.gov/18487275/)

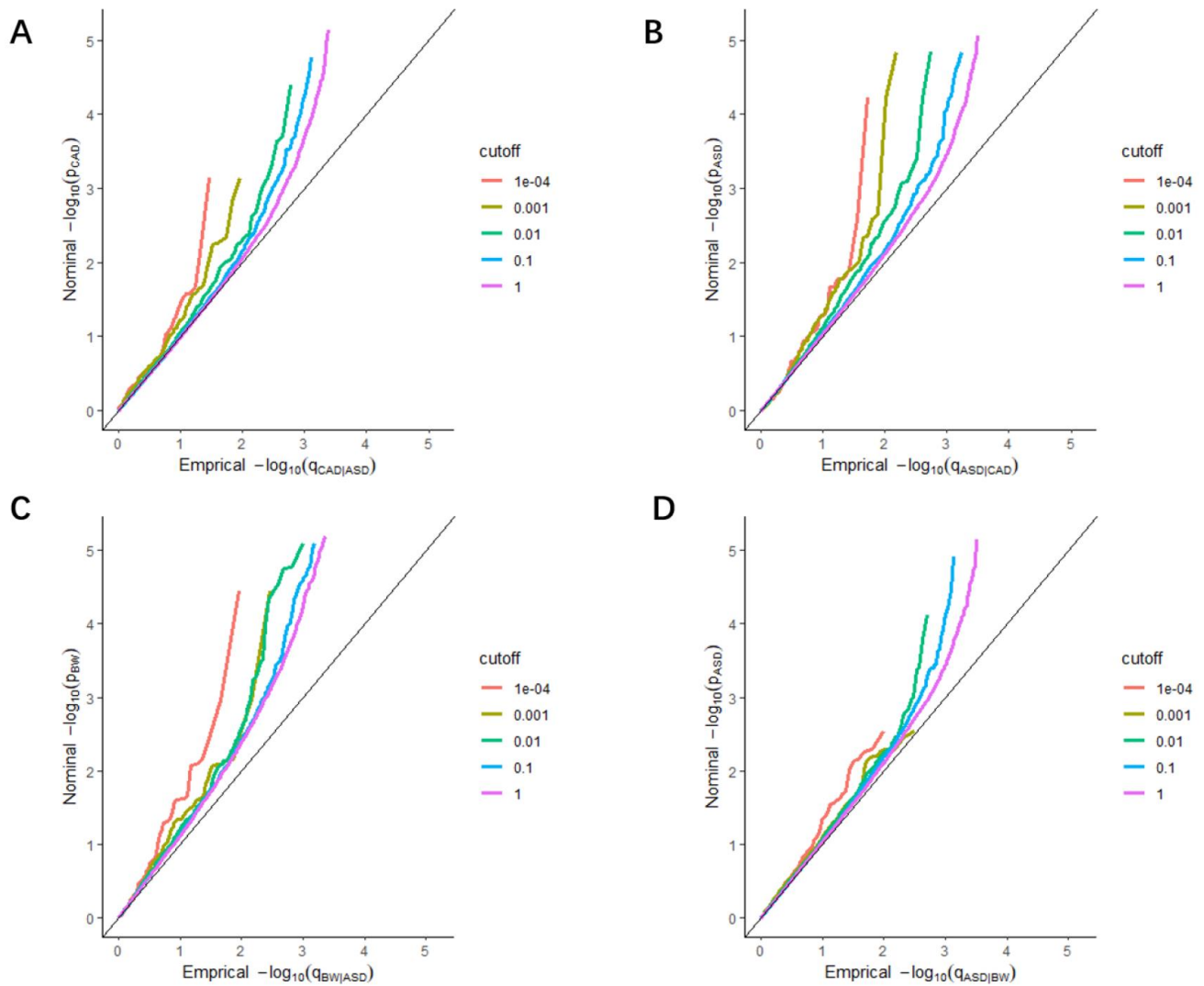
75. Szklarczyk D, Gable AL, Lyon D, Junge A, Wyder S, Huerta-Cepas J, Simonovic M, Doncheva NT, Morris JH, Bork P, Jensen LJ, Mering CV. STRING v11: protein-protein association networks with increased coverage, supporting functional discovery in genome-wide experimental datasets. *Nucleic Acids Res.* 2019; 47:D607–13.

<https://doi.org/10.1093/nar/gky1131>

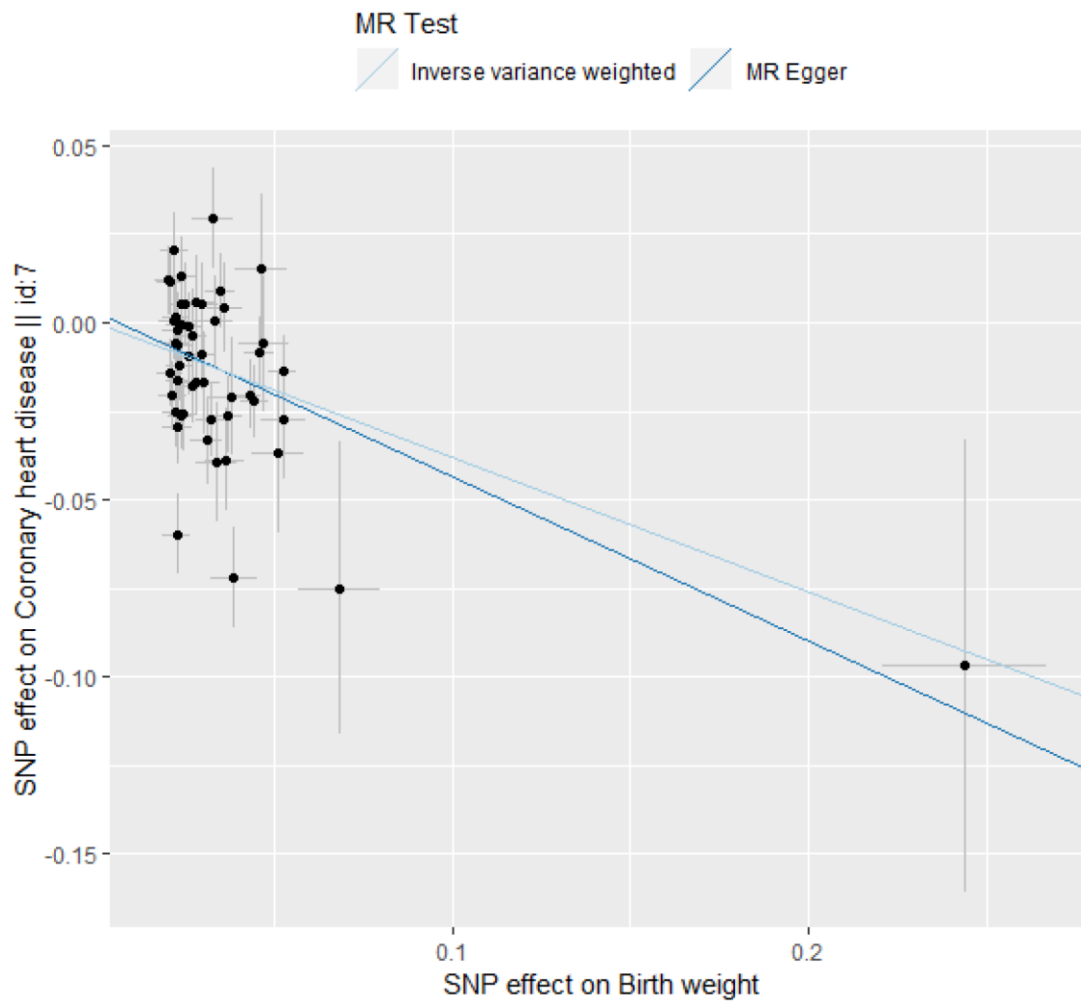
PMID:[30476243](https://pubmed.ncbi.nlm.nih.gov/30476243/)

SUPPLEMENTARY MATERIALS

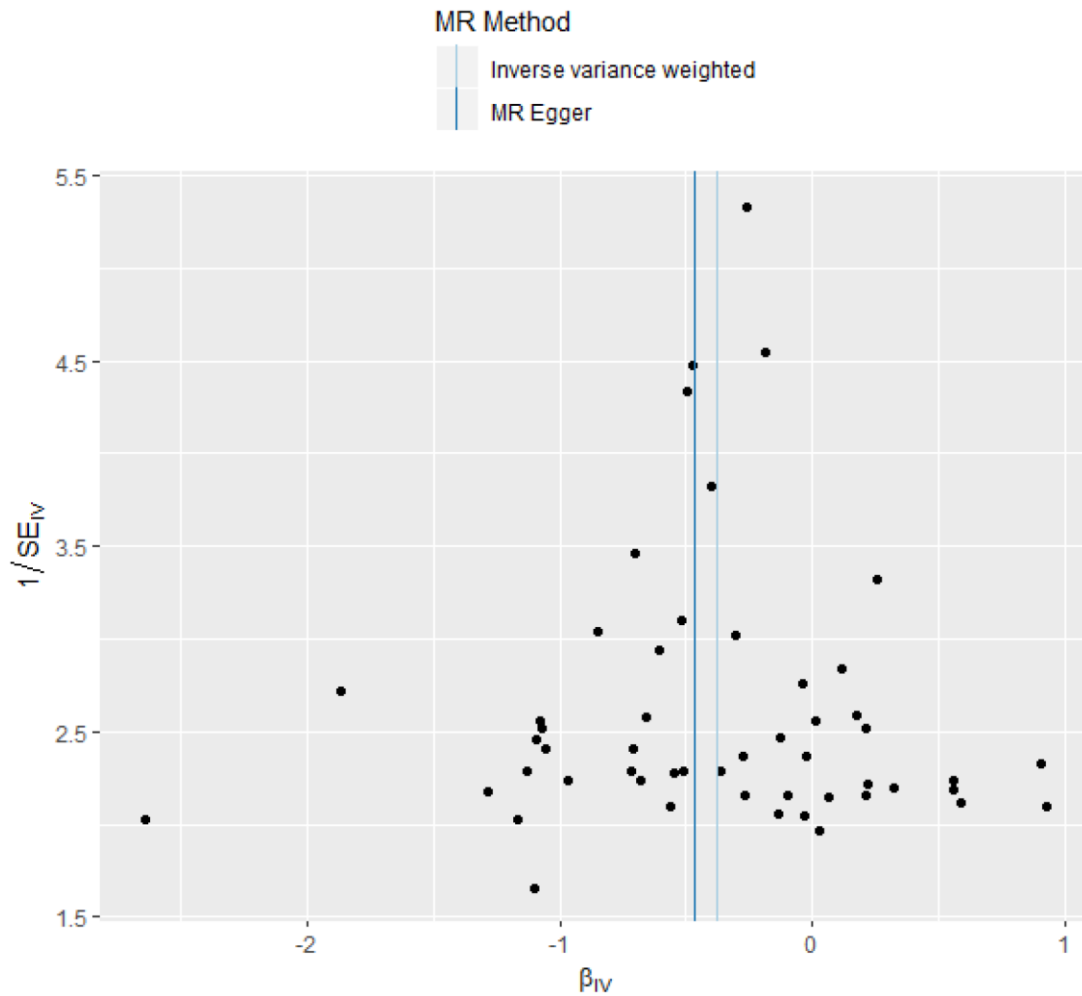
Supplementary Figures



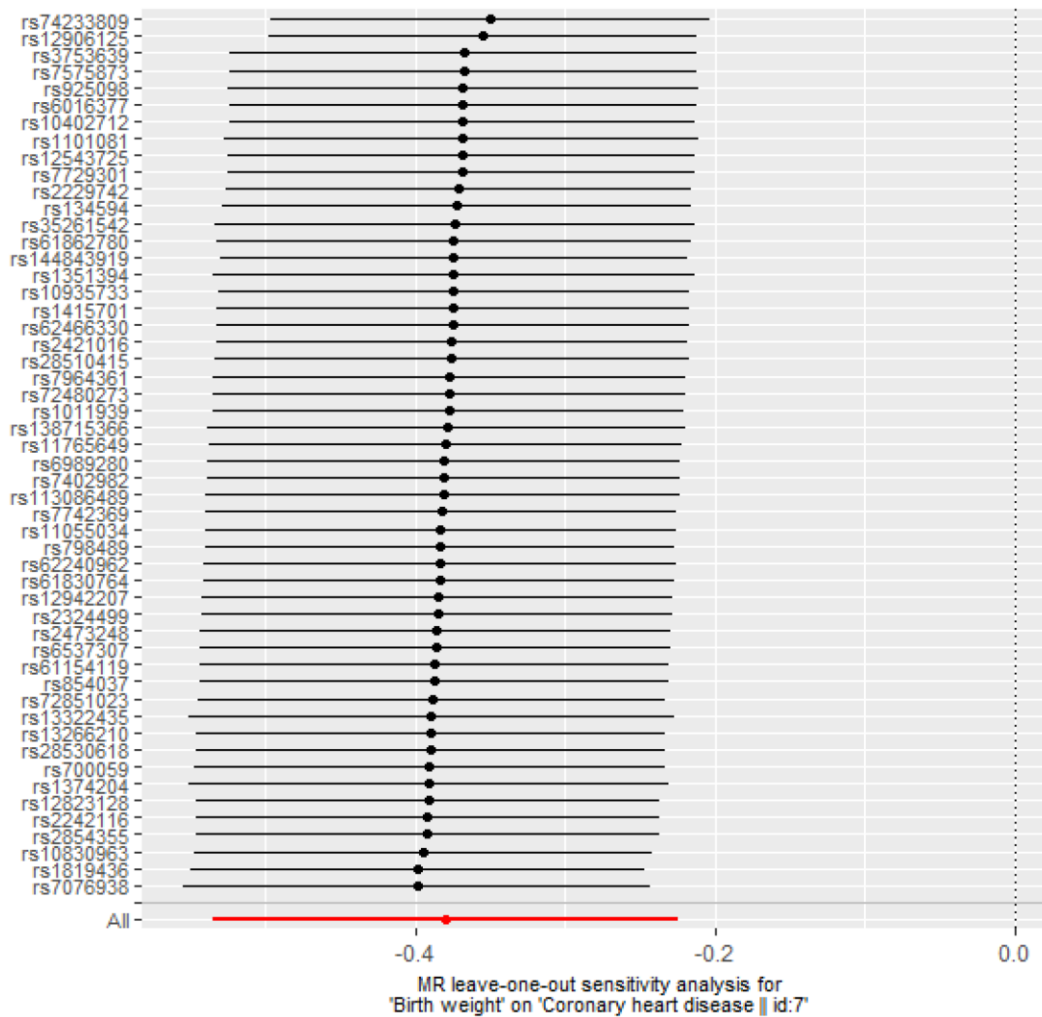
Supplementary Figure 1. Stratified Q-Q plots. Stratified Q-Q plots of nominal vs. empirical $-\log_{10}(p)$ values in principal trait below the standard GWAS threshold of $p \leq 5 \times 10^{-8}$ as a function of the significance of the association with conditional trait at the level of $p \leq 1$, $p \leq 0.1$, $p \leq 0.01$, $p \leq 0.001$, and $p \leq 0.0001$, respectively. **(A)** CAD as a function of the significance of the association with ASD, **(B)** ASD as a function of the significance of the association with CAD, **(C)** BW as a function of the significance of the association with ASD, and **(D)** ASD as a function of the significance of the association with BW.



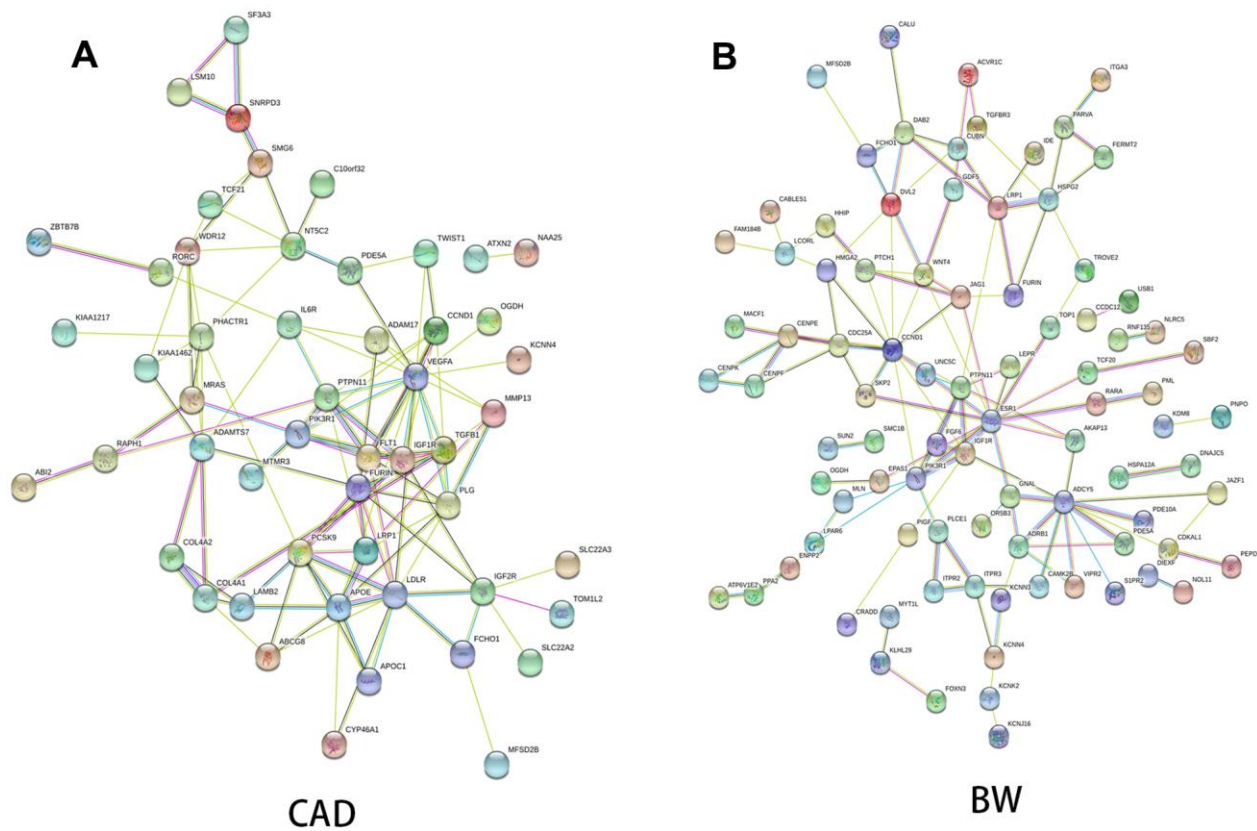
Supplementary Figure 2. MR regression scatter plot. The relationship of the SNP effects on the exposure against the SNP effects on the outcome was depicted using a scatter plot. The different color lines show the results of corresponding MR analysis methods.



Supplementary Figure 3. MR regression funnel plot. Asymmetry in a funnel plot is useful for gauging the reliability of a particular MR analysis. Each SNP's MR estimate is plotted against its minor allele frequency (MAF) corrected association with BW. A MAF correction proportional to the BW related SNP standard error is used since a low-frequency allele is likely to be measured with low precision. Similar to the use of funnel plots in the meta-analysis literature, this plot can be used for visual inspection of symmetry, where any deviation can be suggestive of pleiotropy.



Supplementary Figure 4. Leave-one-out plot. The leave-one-out analysis result was visualized by the forest plot. Each black dot and line correspond to the effect size and 95% confidence interval (95%CI), and the bottom red dot and line is the overall effect size and 95%CI.



Supplementary Figure 5. Functional protein association network analysis. Connections are based on co-expression and experimental evidence with a STRING 10.5 summary score above 0.4. Each filled node denotes a gene; edges between nodes indicate protein-protein interactions between protein products of the corresponding genes in **(A)** CAD and **(B)** BW. Different edge colors represent the types of evidence for the association.

Supplementary Tables

Please browse Full Text version to see the data of Supplementary Tables 1, 3, 4, 6.

Supplementary Table 1. Conditional FDR values of 109 SNPs for CAD given the BW (cFDR \leq 0.05).

Supplementary Table 2. 26 SNPs in high LD ($R^2 > 0.6$) with CAD-associated loci.

SNP	Traits	Proxy SNP	R ²	P_value
rs10781976	Coronary artery disease	rs4888378	0.922	6E-15
rs10818580	Coronary artery disease	rs10818576	0.874	8E-09
rs12044531	Coronary artery disease	rs61776719	0.630	1E-09
rs13070927	Cardiovascular disease	rs2131570	0.992	5E-09
rs1418278	Coronary artery disease	rs10826753	0.692	2E-08
rs1541853	Ischemic stroke	rs7582720	1.000	4E-09
rs2001945	Coronary artery disease	rs6982502	0.988	8E-23
rs2166529	Coronary artery disease	rs6743030	0.926	2E-23
rs2238151	Ischemic stroke	rs10744777	0.995	4E-09
rs2306374	Coronary artery disease	rs185244	0.938	2E-17
rs2812	Coronary artery disease	rs9892152	1.000	6E-11
rs34759087	Coronary artery disease (myocardial infarction)	rs7623687	0.714	4E-10
rs3754211	Coronary artery disease	rs6587520	0.750	9E-09
rs4245791	Coronary artery disease (myocardial infarction)	rs4299376	0.968	6E-10
rs4420638	Coronary artery disease	rs56131196	1.000	2E-14
rs4767293	Ischemic stroke	rs10744777	0.946	4E-09
rs4803455	Coronary artery disease	rs2288874	0.741	4E-16
rs583489	Coronary artery disease	rs518594	0.694	1E-12
rs6922782	Ischemic stroke	rs4714955	0.617	4E-11
rs7164299	Coronary artery disease	rs734780	0.960	4E-10
rs7168915	Coronary artery disease (myocardial infarction)	rs7164479	0.731	6E-18
rs7678	Coronary artery disease	rs6004124	0.929	3E-09
rs7698460	Coronary artery disease	rs13131930	0.720	5E-19
rs93139	Coronary artery disease	rs10840293	0.944	9E-13
rs990619	Coronary artery disease	rs1842896	0.984	1E-11
rs998584	Cardiovascular disease	rs6905288	0.688	1E-12

Supplementary Table 3. Conditional FDR values of 111 SNPs for CAD given the BW in validation dataset in validation dataset (cFDR \leq 0.05).

Supplementary Table 4. Conditional FDR values of 203 SNPs for BW given the CAD (cFDR \leq 0.05).

Supplementary Table 5. 19 SNPs in high LD ($R^2 > 0.6$) with BW-associated loci.

SNP	Traits	Proxy SNP	R²	P_value
rs10786156	Birth weight	rs2274224	0.996	8.00E-13
rs10840346	Birth weight	rs4444073	0.829	3.00E-15
rs1218565	Birth weight	rs6426985	0.832	7.00E-11
rs1319046	Birth weight	rs4965425	0.819	4.00E-09
rs1319859	Birth weight	rs11630479	0.849	9.00E-07
rs1415181	Birth weight	rs1244983	0.733	5.00E-10
rs1983127	Birth weight	rs9645500	0.732	1.00E-12
rs2423512	Birth weight	rs6040076	0.799	7.00E-09
rs2823025	Birth weight	rs2229742	0.814	2.00E-08
rs4812493	Birth weight	rs753381	0.720	3.00E-09
rs5765273	Birth weight	rs11704481	0.662	1.00E-08
rs6007030	Birth weight	rs11704481	0.603	1.00E-08
rs6072263	Birth weight	rs753381	0.724	3.00E-09
rs6918981	Birth length	rs1759645	0.663	7.00E-10
rs7309412	Birth weight	rs2647873	0.877	3.00E-12
rs7846135	Birth weight	rs8180991	0.828	1.00E-08
rs821551	Birth weight	rs670523	0.645	8.00E-12
rs889203	Birth weight	rs2045457	0.779	6.00E-09
rs895964	Birth weight	rs2306547	0.625	4.00E-13

Supplementary Table 6. Conditional FDR values of 229 SNPs for BW given the CAD in validation dataset (cFDR ≤ 0.05).

Supplementary Table 7. MetaQTL effects of significant SNPs.

SNP	Traits	Metabolics	Related disease or biofunctions(PMID)	Sample Type	P_value	Source
rs10774625	Pleiotropic	5-hydroxytryptophan	Depression(31071306)	serum	6.52E-06	SI data (Long et al.)
		hypoxanthine	Coronary artery disease (18651524)	serum	1.29E-06	SI data (Long et al.)
		quinolinate	Acute kidney injury (31055583)	serum	3.21E-06	SI data (Long et al.)
		C-glycosyltryptophan		serum	5.41E-05	SI data (Shin et al.)
		gamma-glutamylleucine		serum	6.14E-05	SI data (Shin et al.)
		kynurenine	Blood pressure (20190767)	serum	1.47E-16	SI data (Shin et al.)
		erythronate	Cirrhosis (29291380)	serum	5.78E-05	SI data (Shin et al.)
rs11066301	Pleiotropic	kynurenine	Blood pressure (20190767)	serum	2.93E-11	SI data (Shin et al.)
		erythronate	Cirrhosis (29291380)	serum	1.71E-05	SI data (Shin et al.)
rs11172113	Pleiotropic	SM C18:1	Coronary artery disease (28431006)	serum	9.21E-05	SI data (Draisma et al.)
rs630014	Pleiotropic	glycylglycine	Alzheimer's disease (28951883)	serum	6.26E-06	SI data (Long et al.)
		ADpSGEGDFXAEGGGVR	T2D (30372032)	serum	3.53E-09	SI data (Shin et al.)
		ADpSGEGDFXAEGGGVR	T2D (30372032)	serum	1.64E-06	SI data (Suhre et al.)
rs10791643	CAD	propylene glycol	Hyperketonemia (27638258)	urine	4.60E-05	SI data (Raffler et al.)
rs11066301	CAD	kynurenine	Blood pressure (20190767)	serum	2.93E-11	SI data (Shin et al.)
		erythronate	Cirrhosis (29291380)	serum	1.71E-05	SI data (Shin et al.)
rs11668477	CAD	cholesterol	Multiple metabolic disease (28319895)	serum	7.69E-05	SI data (Shin et al.)
rs1418278	CAD	X-14057		serum	2.98E-05	SI data (Shin et al.)
rs1541853	CAD	PC aa C32:2		serum	9.24E-05	SI data (Draisma et al.)
rs3811417	CAD	nonanoylcarnitine		serum	9.50E-05	SI data (Shin et al.)
rs3918291	CAD	1,7-dimethylurate		serum	5.41E-05	SI data (Suhre et al.)
rs405509	CAD	X-11820		serum	4.82E-11	SI data (Shin et al.)
rs4245791	CAD	X-12063		serum	3.07E-08	SI data (Shin et al.)
rs445925	CAD	palmitoyl-linoleoyl-glycerol		serum	2.11E-06	SI data (Long et al.)
		17beta-diol monosulfate		serum	2.07E-06	SI data (Long et al.)
		oleoyl-linoleoyl-glycerol		serum	7.34E-06	SI data (Long et al.)
		Tetradecenoylcarnitine	Aging-related Diseases (30498825)	serum	3.00E-05	SI data (Draisma et al.)
		PC aa C28:1		serum	6.54E-06	SI data (Draisma et al.)
		palmitoyl sphingomyelin	Dyslipidemia (18299615)	serum	1.97E-09	SI data (Shin et al.)
		cholesterol	Multiple metabolic disease (28319895)	serum	4.10E-10	SI data (Shin et al.)
rs4895390	CAD	2-hydroxyacetaminophen sulfate	Children obesity (30253079)	serum	8.89E-05	SI data (Shin et al.)
rs624249	CAD	X-12798		serum	2.38E-11	SI data (Long et al.)
rs6922782	CAD	X-12411		serum	6.65E-06	SI data (Long et al.)
rs998584	CAD	SM C16:1		serum	2.76E-05	SI data (Draisma et al.)
rs10221235	BW	PC aa C38:6		serum	1.66E-05	SI data (Draisma et al.)
rs1042725	BW	serine	Multiple metabolic disease (28319895)	serum	7.98E-07	SI data (Shin et al.)
rs10786156	BW	cyclo(leu-pro)		serum	1.26E-05	SI data (Shin et al.)
rs10786706	BW	X-12212		serum	2.68E-05	SI data (Shin et al.)
rs11125079	BW	HWESASXX	Blood pressure (27129722)	serum	7.34E-05	SI data (Suhre et al.)
rs11187076	BW	pregnen-diol disulfate		serum	1.55E-07	SI data (Long et al.)
rs12371967	BW	malate		serum	2.47E-05	SI data (Shin et al.)
rs12656216	BW	lysine	birth weight (19067286)	serum	2.82E-05	SI data (Shin et al.)
rs1389923	BW	hydroxyphenylacetic acid monosulfate		serum	7.18E-06	SI data (Shin et al.)
rs16887484	BW	guanosine		serum	8.82E-07	SI data (Shin et al.)
		inosine		serum	4.51E-05	SI data (Shin et al.)
rs1797081	BW	X-12749		serum	5.74E-05	SI data (Shin et al.)

rs2087826	BW	cotinine		serum	3.39E-05	SI data (Shin et al.)
rs2497304	BW	21-hydroxypregnenolone disulfate		serum	3.37E-06	SI data (Long et al.)
		dehydroisoandrosterone sulfate		serum	8.55E-05	SI data (Shin et al.)
rs3198697	BW	1-dihomo-linolenoyl-GPC		serum	4.53E-06	SI data (Long et al.)
		dihomo-linolenate	Oxidative stress (24760997)	serum	1.56E-07	SI data (Shin et al.)
		1-eicosatrienoylglycerophosphocholine		serum	2.35E-05	SI data (Suhre et al.)
rs3849774	BW	1-(1-enyl-stearoyl)-2-docosahexaenoyl-GPE		serum	8.36E-06	SI data (Long et al.)
rs4428060	BW	ADpSGEGDFXAEGGGVR	T2D (30372032)	serum	5.56E-05	SI data (Shin et al.)
		ADpSGEGDFXAEGGGVR	T2D (30372032)	serum	6.92E-05	SI data (Suhre et al.)
rs4712542	BW	dehydroisoandrosterone sulfate		serum	4.09E-05	SI data (Shin et al.)
rs475931	BW	4-hydroxyhippurate		serum	1.82E-05	SI data (Shin et al.)
rs4812493	BW	ADSGEGDFXAEGGGVR	T2D (30372032)	serum	6.73E-05	SI data (Shin et al.)
rs4875812	BW	deoxycholate		serum	6.12E-05	SI data (Shin et al.)
rs533318	BW	tiglyl carnitine		serum	4.81E-05	SI data (Suhre et al.)
rs6948511	BW	X-11795		serum	3.30E-06	SI data (Shin et al.)
rs8108865	BW	HWESASXX	Blood pressure (27129722)	serum	7.05E-05	SI data (Suhre et al.)
rs889203	BW	3-methylxanthine		serum	9.95E-06	SI data (Suhre et al.)

Supplementary Table 8. 9 pleiotropic SNPs also associated with other phenotypes.

SNP	Chr	Pos	Alt	metaQTL/pQTL/meQTL/eQTL	ccFDR	Traits	PMID
rs10774625	12	111472415	A/T	metaQTL/pQTL/meQTL/eQTL(3 hits)	3.06E-05	Colorectal cancer	29547645
						Hashimoto's thyroiditis	27268232
						Systemic lupus	27906046
						Type 1 diabetes	24936253
						Hypertension	19430479
rs11066301	12	112433568	A/T	metaQTL/meQTL/eQTL(1 hit)	6.50E-03	Hematological parameters	19820697
rs11172113	12	57133500	T/A	metaQTL/meQTL/eQTL(4 hits)	3.18E-02	Headache	29397368
						Migraine	27322543
						Pulmonary function	21946350
rs3756668	5	68300260	G/C		1.32E-02	Type 2 diabetes	29893513
						Small cell lung cancer	28280736
						Endometrial cancer	22146979
rs630014	9	133274306	A/T	metaQTL/meQTL/eQTL(9 hits)	1.16E-02	Pancreatic ductal adenocarcinoma	23816557
						Venous thromboembolism	21463476
						Pancreatic cancer	22523087
rs670950	19	43777410	T/A	eQTL(1 hit)	3.15E-02	Vascular diseases	19644414
rs6713510	2	226169783	G/C		1.29E-02	Fasting plasma glucose	21188353
rs8039305	15	90879313	T/A	meQTL/eQTL(27 hits)	3.77E-06	Hypertension	28686695
rs821551	1	155718789	C/G	meQTL/eQTL(50 hits)	1.08E-02	Osteoporotic fractures	21760914

Supplementary Table 9. Conjunction cFDR for 17 pleiotropic SNPs in CAD and BW in validation dataset (ccFDR ≤ 0.05).

SNP	Chr	Pos	Alt	Gene	Annotation	cFDR.CAD	cFDR.BW	ccFDR	Validation
rs1042725	12	65964567	C/T	<i>HMG2</i>	3'-UTR	1.05E-02	7.21E-29	1.05E-02	No
rs10774625	12	111472415	A/T	<i>ATXN2</i>	intronic	5.16E-12	2.04E-05	2.04E-05	Yes
rs11066301	12	112433568	A/T	<i>PTPN11</i>	intronic	9.98E-05	9.88E-03	9.88E-03	Yes
rs11206803	1	56411837	C/G	<i>AC119674.2</i>	intronic	4.86E-03	4.44E-02	4.44E-02	Yes
rs11853441	15	90856978	T/G	<i>Metazoa_SRP</i>	intergenic	9.38E-03	5.99E-03	9.38E-03	No
rs12306172	12	54145221	G/C	<i>SMUG1</i>	intronic	2.20E-03	1.52E-04	2.20E-03	Yes
rs2243621	6	31464043	C/T	<i>HCP5</i>	3'-UTR	2.56E-02	4.50E-02	4.50E-02	No
rs2339940	2	24028917	G/C	<i>MFS2B</i>	intronic	4.45E-02	1.16E-04	4.45E-02	Yes
rs4233701	2	23706216	G/C	<i>KLHL29</i>	intronic	4.50E-02	1.15E-04	4.50E-02	Yes
rs4704942	5	158466352	G/C	<i>RP11</i>	intergenic	4.95E-02	1.83E-05	4.95E-02	No
rs6016377	20	40544088	C/T	<i>SNORD112</i>	intergenic	2.95E-02	1.83E-07	2.95E-02	No
rs630014	9	133274306	A/T	<i>ABO</i>	intronic	2.05E-03	9.57E-03	9.57E-03	Yes
rs6673081	1	155017119	T/A	<i>ZBTB7B</i>	3'-UTR	3.73E-02	2.11E-07	3.73E-02	Yes
rs6713510	2	226169783	G/C	<i>LOC646736</i>	intronic	1.07E-02	1.63E-02	1.63E-02	Yes
rs8039305	15	90879313	T/A	<i>FURIN</i>	intronic	2.86E-11	3.92E-07	3.92E-07	Yes
rs866919	10	30224354	C/G	<i>RP11</i>	intergenic	3.92E-02	2.45E-02	3.92E-02	Yes
rs965098	21	15185306	G/C	<i>JCAD</i>	intergenic	4.84E-02	4.08E-02	4.84E-02	Yes

Supplementary Table 10. 52 SNPs for genetic association from BW to CAD by mendelian randomization analysis.

SNP	Gene	Alt	BW		CAD	
			<i>P</i>	β	<i>P</i>	β
rs1011939	<i>GPRI39</i>	G/C	3.00E-09	2.36E-02	2.46E-01	-1.20E-02
rs10402712	<i>PEPD</i>	A/T	2.00E-08	2.29E-02	5.33E-03	-2.94E-02
rs10830963	<i>MTNR1B</i>	G/C	1.00E-07	2.20E-02	5.27E-02	2.04E-02
rs10935733	<i>CPA3</i>	T/A	6.00E-10	2.31E-02	8.81E-02	-1.64E-02
rs1101081	<i>ESR1</i>	C/G	6.00E-20	3.70E-02	1.45E-02	-2.61E-02
rs11055034	<i>APOLD1</i>	C/G	2.00E-08	2.30E-02	8.28E-01	-2.32E-03
rs113086489	<i>CLDN7</i>	T/A	1.00E-15	2.96E-02	3.59E-01	-8.98E-03
rs11765649	<i>IGF2BP3</i>	T/A	1.00E-09	2.58E-02	4.07E-01	-9.34E-03
rs12543725	<i>SLC45A4</i>	G/C	2.00E-09	2.23E-02	9.53E-03	-2.52E-02
rs12823128	<i>ITPR2</i>	T/A	3.00E-08	2.04E-02	2.13E-01	1.20E-02
rs12906125	<i>FES</i>	G/C	1.00E-08	2.26E-02	8.64E-08	-5.97E-02
rs12942207	<i>SP6</i>	C/G	3.00E-09	2.38E-02	9.52E-01	-6.04E-04
rs13266210	<i>ANK1</i>	A/T	2.00E-11	2.98E-02	6.57E-01	5.10E-03
rs13322435	<i>CCNLI</i>	A/T	1.00E-42	5.24E-02	1.64E-01	-1.37E-02
rs134594	<i>KREMEN1</i>	C/G	2.00E-08	2.15E-02	3.07E-02	-2.07E-02
rs1351394	<i>HMGA2</i>	T/A	2.00E-33	4.30E-02	3.40E-02	-2.03E-02
rs1374204	<i>EPAS1</i>	T/A	2.00E-29	4.59E-02	3.98E-01	-8.52E-03
rs138715366	<i>YKT6</i>	C/G	1.00E-26	2.44E-01	1.29E-01	-9.68E-02
rs1415701	<i>L3MBTL3</i>	G/C	4.00E-11	2.70E-02	8.78E-02	-1.79E-02
rs144843919	<i>SUZ12P1</i>	G/C	2.00E-09	6.85E-02	6.89E-02	-7.51E-02
rs1819436	<i>RNF219</i>	C/G	2.00E-09	3.29E-02	3.60E-02	2.96E-02
rs2150052	<i>LPAR1</i>	T/A	3.00E-08	2.03E-02	1.75E-01	-1.25E-02
rs2229742	<i>NRIP1</i>	G/C	2.00E-08	3.37E-02	1.82E-02	-3.93E-02
rs2242116	<i>PTH1R</i>	A/T	1.00E-08	2.09E-02	2.21E-01	1.17E-02
rs2324499	<i>LINC00332</i>	G/C	8.00E-09	2.25E-02	8.94E-01	1.39E-03
rs2421016	<i>PLEKHA1</i>	T/A	6.00E-09	2.07E-02	1.27E-01	-1.41E-02
rs2473248	<i>WNT4</i>	C/G	1.00E-09	3.31E-02	9.76E-01	3.83E-04
rs28510415	<i>PTCH1</i>	G/C	4.00E-16	5.26E-02	1.06E-01	-2.74E-02
rs28530618	<i>C20orf203</i>	A/T	8.00E-11	2.40E-02	5.89E-01	5.16E-03
rs2854355	<i>RB1</i>	G/C	2.00E-08	2.40E-02	2.15E-01	1.33E-02
rs35261542	<i>CDKAL1</i>	C/G	1.00E-28	4.44E-02	3.05E-02	-2.21E-02
rs3753639	<i>ZBTB7B</i>	C/G	1.00E-12	3.10E-02	6.05E-03	-3.33E-02
rs6016377	<i>MAFB</i>	T/A	4.00E-10	2.39E-02	7.13E-03	-2.61E-02
rs6040076	<i>JAG1</i>	C/G	7.00E-09	2.18E-02	1.73E-01	1.32E-02
rs61154119	<i>ACTL9</i>	T/A	2.00E-08	2.83E-02	6.48E-01	6.01E-03
rs61830764	<i>DTL</i>	A/T	5.00E-08	2.18E-02	9.62E-01	5.36E-04
rs61862780	<i>HHEX</i>	T/A	1.00E-14	2.79E-02	7.55E-02	-1.69E-02
rs62240962	<i>SREBF2</i>	C/G	4.00E-12	4.70E-02	7.52E-01	-6.01E-03
rs62466330	<i>MLXIPL</i>	C/G	6.00E-12	5.12E-02	9.99E-02	-3.68E-02
rs6537307	<i>HHIP</i>	G/C	1.00E-12	2.59E-02	9.11E-01	-1.05E-03
rs6989280	<i>TRIB1</i>	G/C	5.00E-08	2.21E-02	5.61E-01	-5.95E-03
rs700059	<i>STRBP</i>	G/C	1.00E-12	3.61E-02	7.39E-01	4.23E-03
rs7076938	<i>ADRB1</i>	T/A	5.00E-18	3.49E-02	3.97E-01	8.89E-03
rs72480273	<i>FCGR2B</i>	C/G	2.00E-09	3.00E-02	2.36E-01	-1.70E-02
rs72851023	<i>INS</i>	T/A	7.00E-10	4.63E-02	4.75E-01	1.51E-02

rs7402982	<i>IGF1R</i>	A/T	1.00E-09	2.31E-02	5.19E-01	-6.29E-03
rs74233809	<i>NT5C2</i>	T/A	2.00E-09	-3.87E-02	4.09E-07	7.21E-02
rs7575873	<i>ATAD2B</i>	A/T	6.00E-11	3.62E-02	7.08E-03	-3.87E-02
rs7729301	<i>EBF1</i>	A/T	1.00E-09	2.46E-02	1.12E-02	-2.59E-02
rs7742369	<i>HMGA1</i>	G/C	1.00E-08	2.68E-02	7.87E-01	-3.53E-03
rs7964361	<i>IGF1</i>	A/T	1.00E-08	3.78E-02	2.12E-01	-2.08E-02
rs798489	<i>GNA12</i>	C/G	5.00E-09	2.40E-02	9.54E-01	-6.78E-04
rs854037	<i>Intergenic</i>	A/T	3.00E-08	2.51E-02	6.33E-01	5.40E-03
rs925098	<i>LCORL</i>	G/C	1.00E-15	3.22E-02	1.01E-02	-2.72E-02

Supplementary Table 11. Heterogeneity test assesses whether heterogeneity exists in SNPs.

Method	<i>Q</i>	<i>Q</i> _df	<i>P</i> _value
Fixed effects meta-analysis (simple SE)	121.202	51	0.1804443
Random effects meta-analysis (delta method)	121.202	51	0.1804443
Maximum likelihood	120.8839	50	0.1289658
MR Egger	121.202	51	0.1143716
Inverse variance weighted	119.6123	51	0.1415539

Supplementary Table 12. Causal association from CAD to BW by mendelian randomization analysis.

Method	nSNP	β (95%CI)	<i>P</i> _value
Simple median	39	-0.0002 (-0.0152, 0.0149)	0.98
Weighted median	39	-0.0002 (-0.0253, 0.0250)	0.99
Weighted mode	39	0.0163 (-0.0077, 0.0403)	0.19
Maximum likelihood	39	-0.0002 (-0.0155, 0.0152)	0.98
MR Egger	39	0.0162 (-0.0443, 0.0767)	0.60
Inverse variance weighted	39	-0.0002 (-0.0253, 0.0250)	0.99